United States
Department of
Agriculture

Forest Service

Equipment
Development
Center

Missoula, MT

Experimental Study of Aircraft Wakes in Forest Canopies

PROGRAM WIND
COOPERATIVE ATMOSPHERIC RESEARCH

April 1986
3400—Pest Management
8634 2811

Experimental Study of Aircraft Wakes in Forest Canopies

Prepared by
Guy G. Williamson
Milton E. Teske
Ronald G. Geyer

Continuum Dynamics, Inc.
P.O. Box 3073
Princeton, NJ 08540

DOD
U. S. Army
Dugway Proving Ground

Prepared for
U. S. Department of Agriculture
Forest Service
Equipment Development Center
Missoula, MT 59801

Project Leader
Robert B. Ekblad

April 1986

(This work done under subcontract 85–003 to Geomet Technologies, Inc., February 1985)

Pesticide Precautionary Statement

This publication reports research involving pesticides. It does not contain recommendations for their use, nor does it imply that the uses discussed here have been registered. All uses of pesticides must be registered by appropriate State and/or Federal agencies before they can be recommended.

Caution: Pesticides can be injurious to humans, domestic animals, desirable plants, and fish or other wildlife—if they are not handled or applied properly. Use all pesticides selectively and carefully. Follow recommended practices for the disposal of surplus pesticides and pesticide containers.

FOREWORD

This report is published as a part of the USDA Forest Service program to improve aerial application of pesticides, specifically by using pesticides and delivery systems tailored to the forest environment. The program is conducted jointly by the Equipment Development Center, Missoula, MT, and the Forest Pest Management Staff, Washington Office at Davis, CA, under the sponsorship of State and Private Forestry.

Details of the aerial application improvement program are explained in two Forest Service reports, A Problem Analysis: Forest and Range Aerial Pesticide Application Technology (Equipment Development Center Rpt/7934 2804, July 1979, Missoula, MT) and Recommended Development Plan for An Aerial Spray Planning and Analysis System (Forest Pest Management Rpt. FPM 82-2, February 1982, Davis, CA).

The aircraft wake effect study was cosponsored by the U.S. Army Dugway Proving Grounds and the U.S. Army Chemical Research and Development Center, Research Directorate, Physics Division.

The study was conducted as part of Program WIND (winds in nonuniform domains). Authority for the cooperative program is the Supplemental Agreement, dated February 1985, to the master Memorandum of Understanding Between U.S. Department of Defense and U.S. Department of Agriculture Relative to Cooperation with Respect to Food, Agriculture, and Other Research of Mutual Interest.

A report on Technological Applications and Support Project TE02P18, Technical Services, Forest Pest Management, funded by the Forest Pest Management Staff, State and Private Forestry.

ACKNOWLEDGEMENT

The success of a large ongoing cooperative field study such as project WIND depends on teamwork. This was particularly true in this preliminary study of aircraft wake-forest canopy interaction. Continuum Dynamics, Inc. gratefully acknowledges its debt to the many who made the project possible and successful. Deserving special mention are: Dave Burnham of the Transportation Systems Center of the Department of Transportation for sharing his past experience in wake-vortex measurement and also providing the anemometers used in this project; the pilots who flew the four aircraft with both accuracy and enthusiasm; Tom Efird and the staff of the Foresthill Ranger Station for their aid in erecting instrumentation towers; Jim Keetch and Keith Dumbauld of Dugway Proving Grounds for smoothly running the tests at the orchard site; Jim Kautz of the Forest Service for manning the cameras and helping wherever needed; Jim Bergen of the Forest Service for loaning us instrumentation and tower sections; Bob Ekblad and Jack Barry of the Forest Service for both their on site assistance and valuable guidance throughout the project.

TABLE OF CONTENTS

LIST OF ILLUSTRATIONS

LIST OF ILLUSTRATIONS (Cont'd)

1. SUMMARY OF EXPERIMENTAL FIXED- AND ROTARY-WING AIRCRAFT WAKE FLOW FIELD STUDY

(Improved Wake Effects Module - Task IV)
Part of Program WIND

1.1 Background

The first phase of program "Winds in Nonuniform Domains" (WIND) was performed jointly by the United States Department of Agriculture Forest Service and the United States Army at several sites in northern California from May through July of 1985. A specific objective of the Forest Service in this program is to evaluate and improve the ability of selected spray dispersion models to predict the deposition and drift of liquid sprays in flat and moderately complex forest and rangelands.[1]

Two of the models for the dispersion of the spray released from aircraft are implemented in the computer codes AGDISP (AGricultural DISPersal)[2] and FSCBG (Forest Service Cramer-Barry-Grimm).[3] In the code FSCBG, it is assumed that the spray from the aircraft has had time to form a plume with Gaussian characteristics prior to ground contact as in the case of high altitude release of chemicals. For this case, the wake-canopy interaction is not relevant. However, when the spray is released at low enough altitudes, the wake vortices will penetrate the forest canopy and will affect the distribution of the spray on the ground and trees. It is, therefore, desirable to understand the aircraft wake-forest canopy interaction as a first step in predicting the deposition distribution of sprays. The code AGDISP[2,4,5] models both the wake flow of fixed- and rotary-wing aircraft and the interaction of this flow with the forest canopy. The AGDISP code has had experimental validation[6] with no canopy present. As a first step it was, therefore, necessary to measure the wake flow within a forest canopy in order to refine and evaluate models of this interaction. The choice of method to accomplish this relied heavily on past efforts of the Transportation Systems Center of the Department of Transportation to measure aircraft wake flows at the end of runways.[7,8,9] Various methods of velocity measurement, based on the Doppler frequency shift, had proven quite successful. The cost of these

systems and the effects of the forest canopy made them less attractive for this test program. The Transportation Systems Center had determined that a grid of propeller anemometers attached to towers erected in a line perpendicular to the runway could detect the presence of vortices if they were sufficiently strong and low in altitude. This method seemed well suited to the needs of this program, since the wake flow would be just above or in the forest canopy, and the anemometers could be erected on towers just clearing the top of the canopy. (This method was also used in a prior orchard spraying study.[10]) However, the strength of the vortex filaments produced by the aircraft used for spraying is much less than that produced by commercial jets. The primary goal for this test program was, therefore, to evaluate this method of measuring the wake flow field generated by these lightweight aircraft with and without light crosswinds present. The anemometers used were loaned by the Transportation Systems Center to the Forest Service for this program.

This system for measuring aircraft wake flows at low altitude was adapted for use in forest canopies as a field study performed jointly by the Forest Service and Continuum Dynamics, Inc. in program WIND. The work performed by Continuum Dynamics, Inc., under contract to GEOMET Technology, Inc., was funded through the United States Army, Dugway Proving Grounds. Program WIND is conducted under the February 1985 Supplemental Agreement to the master memorandum of understanding between the U.S. Department of Defense and the U.S. Department of Agriculture relative to cooperation with respect to food, agriculture, and other research of mutual interest.

1.2 Long Term Objective

The long term objective is to develop a validated methodology capable of predicting the deposition and drift of aerially applied sprays in canopies. This methodology will predict distribution of dosage on the vegetation and ground as a function of:

1) aircraft type and operating conditions,
2) meteorological conditions, and
3) canopy type.

1.3 Current Objective

The current objective is to demonstrate that rather simple instrumentation can be used to obtain data needed to develop an aircraft vortex wake-canopy interaction model.

Specific tasks:

1) develop instrument placement methodologies and data reduction algorithms to quantify the vortex flow field in a forest canopy,

2) determine the degree of vortex penetration into the coniferous canopy at Foresthill Seed Orchard and the broadleaf canopy at the Hennigan Almond Orchard, and

3) determine the amount of additional instrumentation, testing and data processing required to provide a data base adequate to develop a wake-canopy interaction model.

1.4 Program Description

A line of seven towers with three levels of anemometers was erected at three different test sites (Section 2) in order to measure the evolution of the wake flow generated by aircraft during simulated and actual aerial application of liquid sprays. The variable height towers were first erected 45 ft high in an open field at the Foresthill Seed Orchard in order to obtain reference wake data without the influences of a forest canopy. The test vehicles (Section 2), a Cessna Ag Husky fixed-wing aircraft and a Bell 206 rotary-wing aircraft, made a total of 58 early morning flights over the instrumentation (Section 3) at various speeds, altitudes and weights (Section 5). The instrumentation was then moved into the Ponderosa pine canopy some 800 ft southwest of the open field site at the Foresthill Seed Orchard. Here the towers were extended to a height of 55 ft. The same two aircraft made a total of 71 flights over the instrumented grid.

The towers, anemometers, data acquisition system, etc., were then moved to the Hennigan Almond Orchard test site north of Chico where the distributions of dyed water sprayed from a Schweizer Ag Cat fixed-wing aircraft and a Hiller UH-12E rotary-wing aircraft were measured by personnel from the U.S. Army Dugway Proving Grounds and their subcontractor Lockheed. The towers were set just beyond the distribution measurement area so that the aircraft passed over the anemometer grid just after completing each spray pass. A total of 109 passes were made by the two aircraft over the instrumented grid at various speeds, weights and lateral positions.

Preliminary on-site data reduction confirmed that for many of these tests wake-vortex behavior was easily discerned. This indicated that the instrumentation grid, while not optimum, was at least adequate for obtaining preliminary data useful for modeling the vortex-canopy interaction. As a result, data were taken on a larger number of flights than originally anticipated. However, reduction of most of these data and the development of wake-canopy interaction models remains as a future task. In post test data analysis an algorithm was developed to identify the position and strength of the vortex pair which produced the velocities measured on the grid at each instant in time (Section 6). This data reduction algorithm has been applied to representative sets of data for both fixed-and rotary-wing aircraft at all three test sites (Section 7). Agreement with analytic predictions for open field tests is good and the anticipated dissipation of the vortices in the canopies is observed.

1.5 Conclusions and Recommendations

The major conclusions and recommendations from this study are given below.

1) A two-dimensional grid of appropriately located anemometers can provide a description of the wake flow field for fixed- and rotary-wing aircraft under flight conditions for spray applications, useful for modeling the vortex-canopy interaction, providing that the initial vorticity is sufficiently intense.

2) Most of the anemometers in the grid should be oriented vertically in order to avoid the measurement errors introduced by the ambient crosswind on the horizontal wake flow velocity component measured by horizontally oriented anemometers.

3) The instrumentation grid should extend further laterally (more towers) in order to track the wake flow for a longer period of time under normal operational crosswind conditions.

4) The data reduction algorithm should be extended to include more complex wake flow field models to account for vortex tipping and rotary-wing aircraft operating at low advance ratios.

5) Preliminary models of wake vortex dissipation due to forest canopy interaction should be developed using the existing data base.

2. TEST EQUIPMENT AND FACILITIES

The aircraft and test sites comprise the noninstrumentation components of this test program and are described in this section.

2.1 Test Aircraft

At each test site one fixed-wing aircraft and one rotary-wing aircraft were flown over the anemometer grid. At the Foresthill open field and forest sites, the aircraft used were a Cessna Ag Husky owned by Gilbert Aviation Industries and a Bell 206 owned by Chuck Jones Flying Service. The Ag Husky flew out of Auburn Airport and was in radio contact with the ground crew. The helicopter had limited radio contact with the ground crew and, therefore, landed in the open field after every three to six runs to receive instructions for the next few tests.

The aircraft tested at the orchard site were a Schweizer Ag Cat biplane and a Hiller UH-12E helicopter both owned by the Chico Aerial Applicators. The aircraft were flow out of the Chico airport and were in radio contact with the test conductor. The aircraft were flown with different loads of water depending on the spray rate used in the test sequence. Table 2-1 lists the relevant physical properties of the aircraft used in this test program.

2.2 Test Sites

2.2.1 Tests were first performed in a cleared field at the Foresthill Seed Orchard in Tahoe National Forest near Foresthill, California (Figure 2-1). The field is located on the Foresthill Divide with a ridge line running downhill in the southwestern direction. This ridge characteristic resulted in significant drainage winds during testing (the period of least wind variability but with adequate light for flying, 5:30 a.m. to 8:00 a.m.).

TABLE 2-1

Test Aircraft Data

Manufacturer	Model	Owner	Test Weight Range (lbs)	Wing/Rotor Span (ft)
			Light - Heavy	
Bell	206 Jet Ranger	Chuck Jones Flying Service	2100 - 2700	37 33⅓
Cessna	Ag Husky	Gilbert Aviation Industries	2600 - 4000	41.7
Hiller	UH-12E	Chico Aerial Applicators	2600 @ 19 mph	35
Schweizer	Ag Cat	Chico Aerial Applicators	4000	42.5

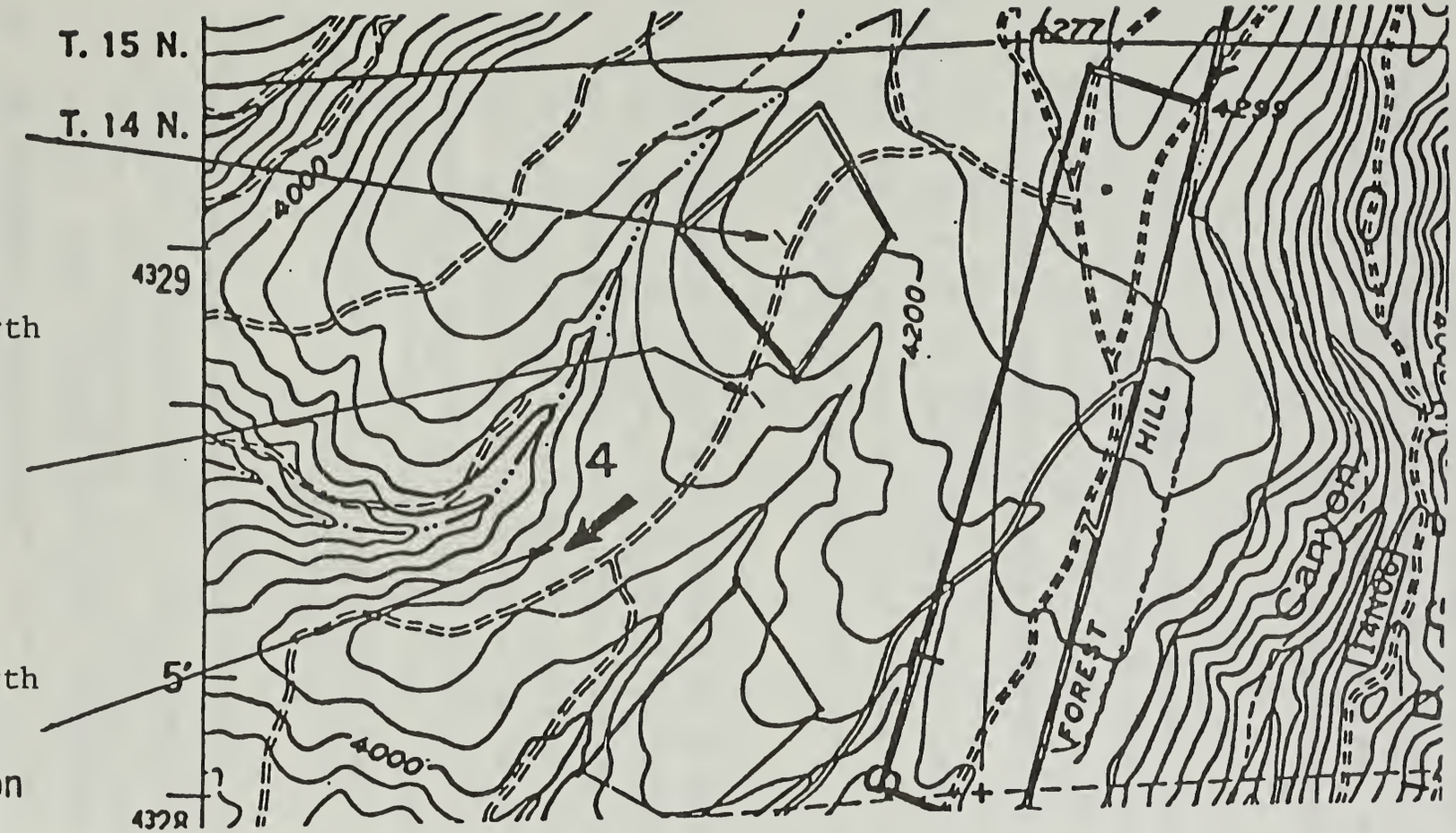

Figure 2-1. Foresthill Seed Orchard test site from Primary Base Series Map FS No. 540-3C.

The line of instrumented towers was, therefore, set up (145° from north) perpendicular to this anticipated wind in order to minimize the crosswind and thereby keep the vortices in the instrumented towers for the maximum amount of time.

2.2.2 The second set of tests was performed in the forest about 300 ft in from the southwest side of the open field (Figure 2-1). The forest canopy consists of 25-year old Ponderosa pines planted at a density of 225 trees/acre (about 15 ft apart). The trees are approximately 50 ft tall, have a 1-1/2 ft base diameter, an active crown in the upper half of the tree and with the longest branches of adjacent trees touching.

Meteorological data taken early in June indicated that the drainage wind in the forest at the two-meter level was from nearly due north. The prevailing winds above the canopy were more easterly. The line of towers was, therefore, set up perpendicular to the prevailing winds at the 50 ft altitude within the constraints imposed by the forest. The actual line chosen which required minimum forest damage due to tower installation was 150° from north (Figure 2-1).

2.2.3 The third site for testing was the Hennigan Almond Orchard located north of Chico which was heavily instrumented to obtain both meteorological and actual spray distribution data for project WIND (Figure 2-2). Orchard characteristics are well documented in References 11 and 12.

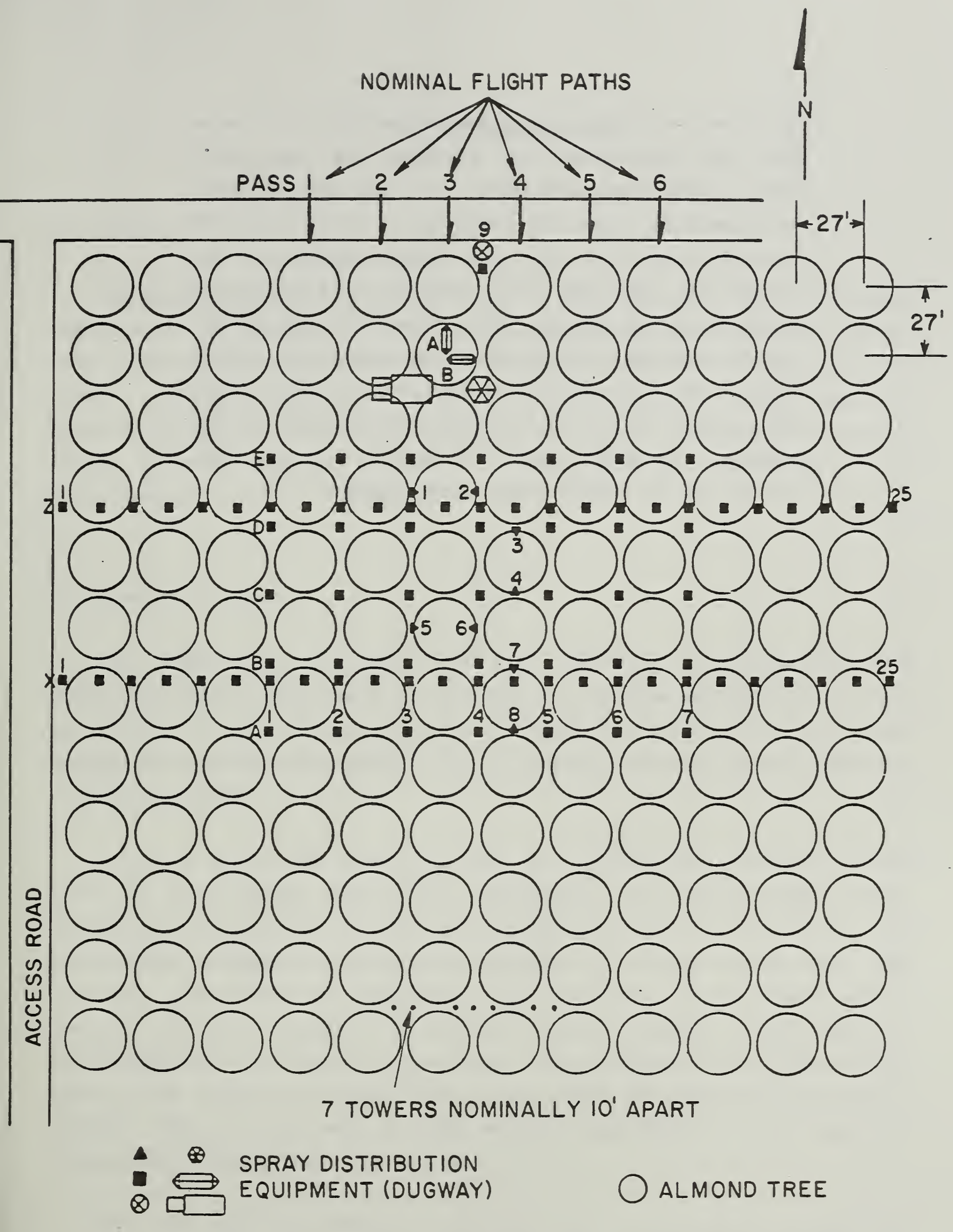

Figure 2-2. Anemometer tower locations at Hennigan Almond Orchard test site.

The trees are planted in a square pattern 27 ft on a side, are approximately 25 ft high, and touch each other at their maximum diameter. At this time of year, the prevailing winds are northerly if it is cool and southerly when hot. The test program called for the aircraft to fly over the orchard in a southerly direction at all times. The towers were, therefore, erected in an east west direction perpendicular to this flight path. The row of towers was located eleven rows, or 297 ft, south of the northern edge of the orchard. The middle tower was located six rows east (162 ft) of the western edge of the orchard.

3. TEST INSTRUMENTATION

3.1 General

The primary instrumentation consisted of a vertical grid of tower-mounted anemometers with the wake velocity signals sampled and recorded with a digital data acquisition system, prior, during and after the aircraft flight over the towers. Aircraft altitude was measured photographically. Ground speed was measured by Doppler radar and photographs and video recordings were taken of vortex patterns whenever possible. A more detailed description of the instrumentation system is given below.

3.2 Anemometer Towers

The towers used to mount the flow measuring instrumentation were telescoping masts which could be extended to a maximum height of 45 ft. At all sites, the towers were placed in a single line (within the constraints imposed by the trees) perpendicular to the prevailing early morning (5:00 a.m. - 8:00 a.m.) winds.

A pilot's view of the open field test site is sketched in Figure 3-1 along with the axis system used in the description of aircraft flight paths, instrumentation locations and the presentation of wake velocity data. An earth-fixed, orthogonal axis system with origin at the base of the center pole is used. The x-axis is perpendicular to the plane of the towers and is positive in the direction of aircraft forward motion. The y-axis is horizontal and in the plane of the towers and is positive to the right of the pilot. The z-axis is vertical and in the plane of towers and is positive upwards. The x, y and z wake velocity components u, v and w, respectively, follow these conventions.

Note that the axis system is dependent on the direction in which the aircraft flies over the towers. There were seven towers erected at each of the Foresthill sites; spaced twenty feet apart and numbered 1 - 7 from left to

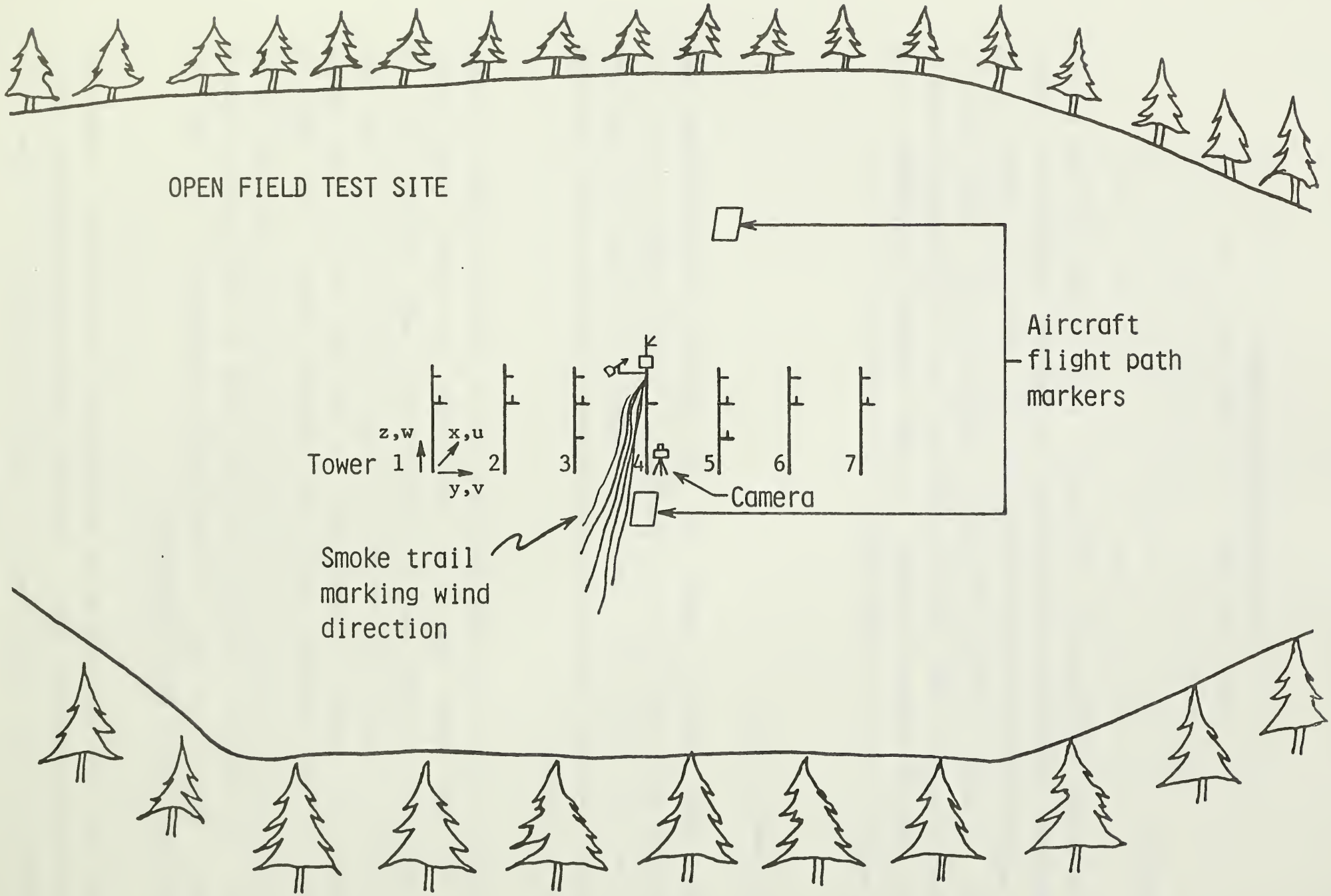

Figure 3-1. Pilot's view for open field test.

right, as the pilot views them. The rationale behind this tower spacing along with the vertical spacing of the anemometers is given in Section 3.3.

In the forest, it was necessary to raise the masts 10 ft to an altitude of 55 ft in order to make flow measurements above most of the trees. This was accomplished by mounting each telescoping mast on top of a 10 ft tower segment. Branches were removed from some of the trees to facilitate tower erection. In no case was the top third of the trees disturbed.

The almond trees in the orchard averaged 27 ft high and were spaced 27 ft apart. Seven towers were erected using the telescoping masts extended to 28 ft and spaced approximately 10 ft apart.

3.3 Anemometers

Gill anemometers manufacturered by the R.M. Young Company, on loan to the U.S. Forest Service from the Transportation Systems Center of the U.S. Department of Transportation were used for this study. Four-bladed propellers (mostly 19 cm in diameter) were coupled with the DC generators to complete the anemometer. The anemometers were mounted on the towers in pairs oriented horizontally and vertically in the plane of the tower in order to measure the crosswind velocity (Figure 3-1). In addition, the velocity component, u, along the flight path was measured at the top location of the middle tower. This was primarily used to relate ground speed to airspeed for comparison with theoretical predictions.

The actual and ideal outputs of an anemometer are plotted in Figure 3-2 as a function of wind angle to the propeller spin axis. It is seen that the anemometer slightly underpredicts the magnitude of the wind along the spin axis. When operating in orthogonal pairs, it can be shown that the maximum error in magnitude of velocity occurs at an angle of 45° and is an underprediction of 13%. However, this error can be eliminated by iterating to find the actual values of velocity. Data reduction has been performed with and without this correction and is discussed in Section 6.4.

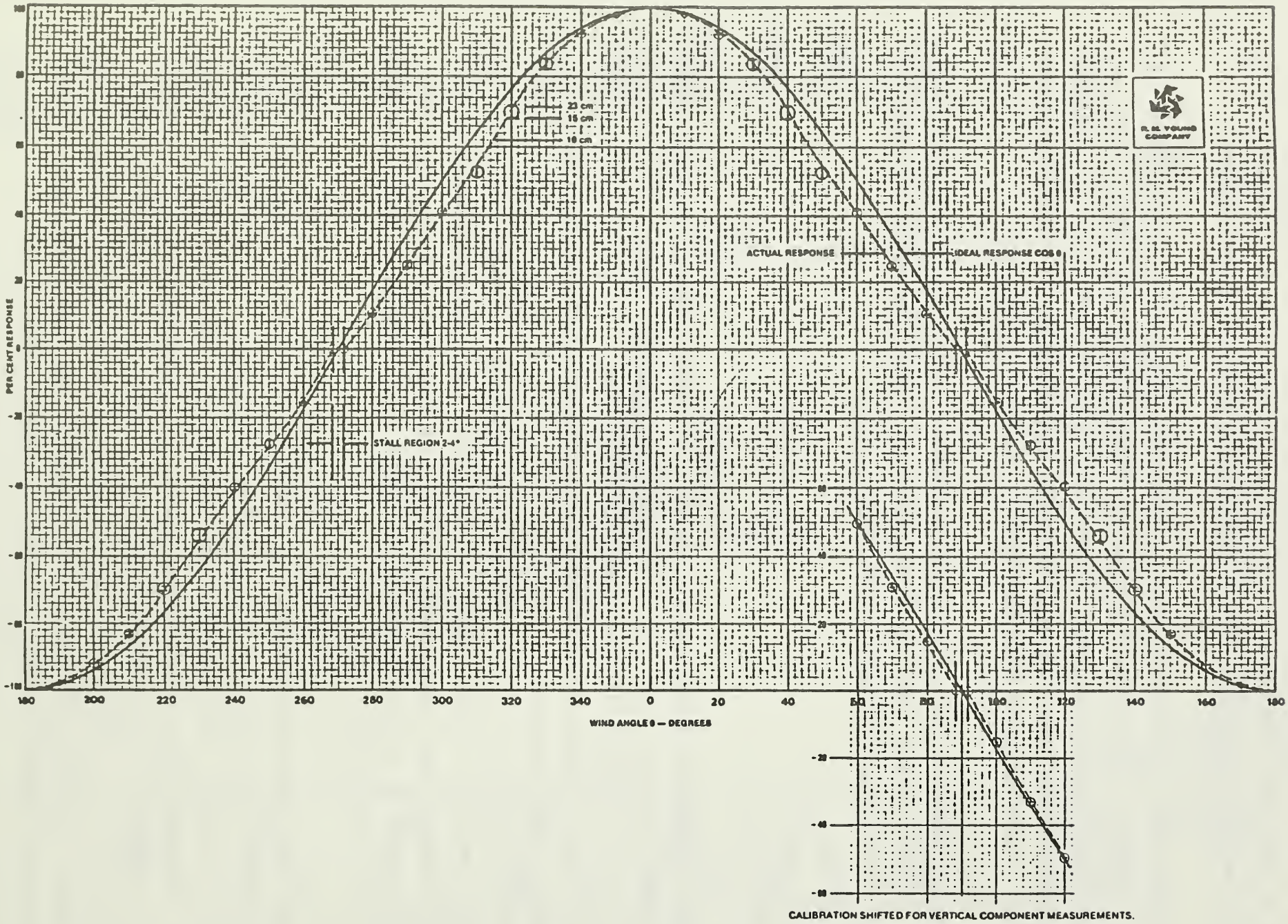

Figure 3-2. Propeller response versus wind angle. Actual signal output versus ideal signal at all wind angles.

The wind velocity component, u , perpendicular to the plane of the towers will also result in velocity estimation errors. However, for the data presented in this study, the magnitude of the longitudinal velocity is small compared to that of the major crosswind generated by the aircraft.

The anemometers were mounted on the masts at three heights. Not all masts had anemometers mounted at the lowest position. Also, due to the 32-channel limit on the data acquisition system (Section 3.4), not all of the anemometers were monitored on the same flight. Flights were, therefore, repeated with anemometers at different locations monitored in order to determine the most efficient anemometer spacing. The different anemometer grids which were used are shown in Figure 3-3. The anemometer grid used on each flight is listed in Table 5-1. Note that the grid spacing in the orchard is much closer since the almond trees are shorter and all flights were at a lower altitude (40 ft).

The anemometers were electrically connected to the data acquisition system with filtering capacitors in accordance with the manufacturer's recommendations in order to attenuate the voltage ripples resulting from the brushes contacting different armature segments in the generator.

3.4 Data Acquisition System

The data acquisition system consisted of an IBM PC with two Data Translation 2801 auxiliary boards to sample and digitize 32 channels of analog voltage signals from the anemometers (Figure 3-4). Sampling was carried out at a rate of 100 samples/sec (each anemometer was sampled every 0.32 sec). The full scale analog voltages -/+ 1.25 volts were converted to the digital representations 0/4096, respectively, and stored in memory. Over one minute's worth of data could be sampled continuously and stored for post test conversion to engineering units and further analysis.

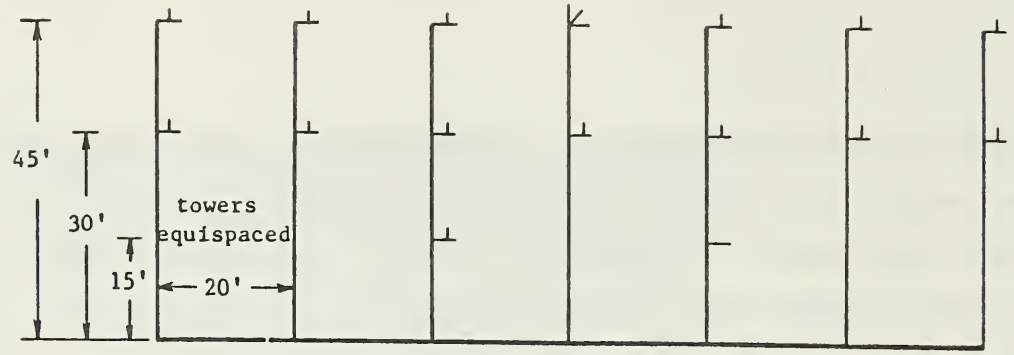

GRID A - Open Field

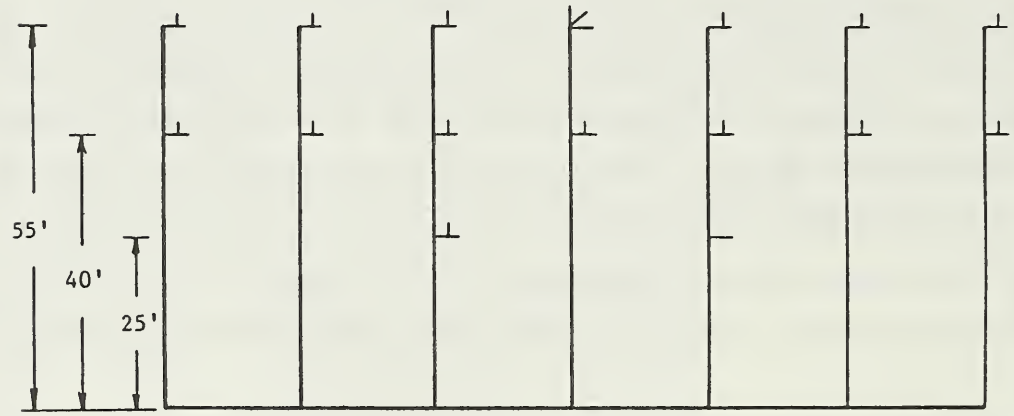

— denotes 1 axis anemometer

⊥ denotes 2 axis anemometer

GRID B - Forest

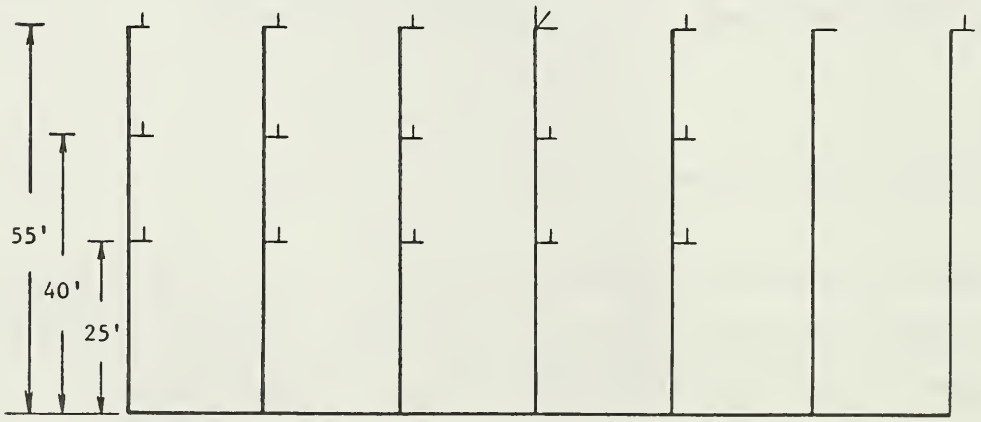

denotes 3 axis anemometer

GRID C - Forest

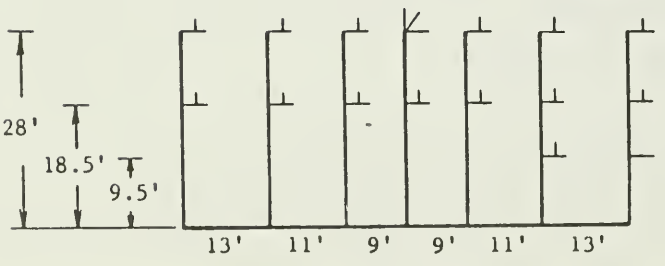

GRID D - Orchard

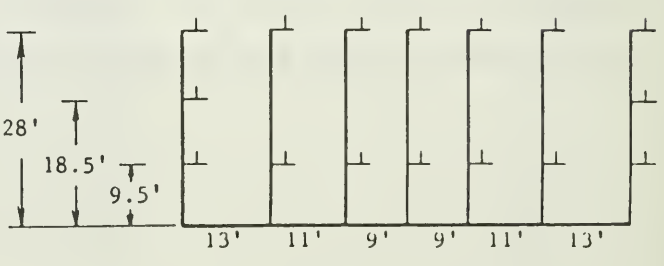

GRID E - Orchard

Figure 3-3. Anemometer grids used for wake velocity measurements (1" = 30.5').

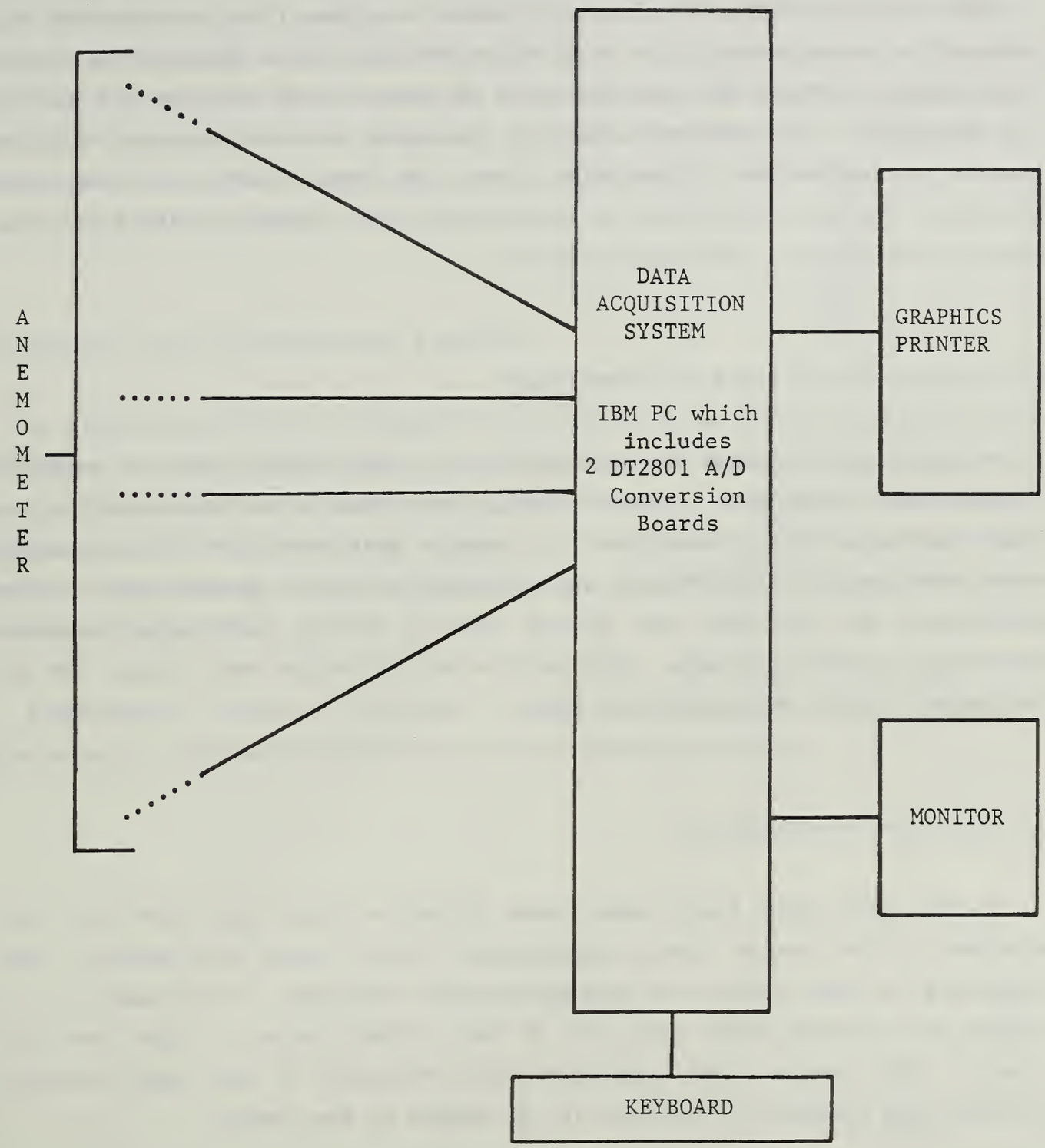

Figure 3-4. Instrumentation schematic for wake flow field tests.

3.5 Aircraft Altitude Measurement

The altitude of the aircraft as it passed over the grid of anemometers was measured by photogrammetry. A vertically oriented 35 mm Nikon with electric film transport (Figure 3-1) took pictures of the aircraft flyby at the rate of six frames/sec. The apparent length of the spray boom was compared with the length in calibration photographs taken at known distances from each aircraft. The lateral position of the aircraft with respect to the towers can also be obtained from these photographs.

3.6 Aircraft Ground Speed and Measurement

Aircraft ground speed was measured using a U.S. Forest Service supplied Doppler radar speed gun. In most cases, the operator was positioned in the flight path of the aircraft and far enough away that the line of sight measurement was a satisfactory approximation of true ground speed. The calibration of the unit was checked with a tuning fork with frequency simulating a speed of 50 mph. This particular unit worked well except for the helicopter flights at less than 20 mph.

3.7 Wake Flow Visualization

In the open field tests smoke bombs (Superior Signal Co. Model 5D) were attached to the center tower approximately 40 ft above the ground. The trajectory of this smoke was photographically recorded. The camera, on a tripod, was located under the path of the aircraft after it flew over the towers. With proper wind conditions the trajectory of the smoke visually confirmed the presence of vortices in the region of the towers.

Superior Signal Co. Model 5D smoke bombs were attached to the spray boom of the helicopter to aid in tracking the wake vortices. The volumetric rate, optically obscured by the smoke, 20,000 ft^3/min, was too low to visualize any more than the first spiral of the smoke in the vortex.

The tests run in the orchard included actual spraying with water containing Rhodamine dye to experimentally determine the distribution of the spray in the broadleaf canopy. Ground observation from behind the aircraft during the spraying operation indicated that the dye aided in visually defining the interaction of the spray with the wake flow. Video recordings were made by Dugway/Lockheed personnel from an elevated station just east of the flight path. These recordings may visually depict the trajectory of the spray in a useful fashion.

3.8 Ambient Wind and Temperature Profiles

An altitude profile of the ambient wind was made at the beginning and end of testing each day at Foresthill. A Thermo Systems Inc. hot film anemometer was carried beneath a tethered helium filled weather balloon. Measurements were made at 20 ft intervals up to 100 ft. In addition, the temperature was recorded continuously at two altitudes (6 ft and 30 ft) during most of the testing at Foresthill.

Atmospheric Sciences Laboratory (ASL) recorded much more extensive meteorological altitude profile data at the orchard test site.

4. TEST PROCEDURE

The procedures followed during testing were practically the same at all three test sites. A single review is, therefore, given below with site specific variations included.

Personnel arrived on site prior to sunrise for each day's testing. The computer was connected to the anemometers and battery power and the DAS system was checked out. Ambient wind conditions were measured using site specific meteorological instrumentation and observed with the aid of smoke. The aircraft arrived around 6:00 a.m. for the start of testing. The test coordinator would relay the desired flight conditions to the pilot who would then fly over the desired tower based on the crosswind conditions. The computer operator would initiate the data acquisition sequence based on visual contact with the aircraft. The test coordinator, standing in the line of towers, would take a burst of pictures with the vertically oriented camera to document the altitude and lateral position of the aircraft as it passed over the towers. The radar gun operator, stationed in the open field in the ground track of the aircraft, would record the ground speed as it passed over the towers. The pilot would then fly a large circular pattern until up to a minute's worth of wake flow data were recorded and transferred to floppy disk storage (a total of two minutes). The cycle was then repeated for the next set of flight conditions in the test matrix.

In the open field tests, head-on still photographs were taken by U.S. Forest Service personnel of the aircraft as it flew over the towers and also of the flow patterns which developed afterwards from the interaction of the tower mounted smoke bomb and the wake flow field.

In the tests run at the orchard site, the computer operator initiated data acquisition when the flagman signaled that the aircraft was over the orchard. Video recordings were made by Dugway/Lockheed personnel of the Rhodamine dye sprayed from the aircraft. These recordings should graphically depict the effect of the wake vortices on the spray trajectory in particular when there was only a light crosswind.

5. TEST MATRIX

The primary objective of this test program was to determine if satisfactory data could be obtained from a simple two-dimensional grid of anemometers to define the wake flow from agricultural aviation aircraft. The likelihood of success increases as the circulation strength, Γ , increases. This variable can be expressed in terms of more physically meaningful parameters, air density, weight and velocity as:

$$\Gamma = \frac{W}{\rho U \hat{b}}$$

where $\hat{b}$ = distance between centroids of vorticity.

To obtain the largest circulation strength it is desirable to fly with the aircraft as heavy as possible and as slow as possible within normal safe operation limits. Two parameters to be varied in the test matrix were, therefore, payload weight and aircraft speed.

Payload weight was varied by the amount of water and fuel on board each flight. In the tests at Foresthill, the aircraft flew with water in the tanks for roughly the first two-thirds of the tests each day and then discharged the water for the remaining third of the day's tests. In the tests conducted at the orchard site, the aircraft would make several passes over the center tower without spraying and would then spray the area in six passes at the specified rate reducing its weight continuously.

All of the aircraft were flown at the slowest velocity used for spray operations in order to maximize the strength of the circulation in the wake flow. In addition, three of the aircraft were flown at two higher velocities in the range normally used for spray operation in order to obtain data on wake flows with lower circulation strengths. The Ag Cat was flown at one higher speed. Altitude was also varied in the tests run at Foresthill in order to obtain data on the interaction of the canopy with the wake in different stages of vortex roll-up. The normal low altitude passes were with the aircraft

spray boom approximately 15 ft above the tops of the towers and the high altitude passes were an additional 15 ft above that height. All tests conducted at the orchard site were run at an average altitude of 40 ft above the ground.

Test flights at the forest site were flown in the north easterly direction going uphill (as in the open field tests) and in the opposite (downhill) direction to avoid the glare of the sun and to line up more accurately the markers in the open field prior to flying over the towers. This was the only test site at which the aircraft flew over the anemometer grid in both directions.

A complete listing of the tests is contained in Table 5-1 in chronological order. Test description (qualitative altitude, speed and weight) as well as measured altitude and speed are given, along with the anemometer grid connected to the DAS as defined in Figure 3-3.

TABLE 5-1

Date	Location	Aircraft	Flight No.	Description	Altitude (ft)	Ground Velocity (mph)	Instrument Grid
6/6/85	Open field	Bell 206	F005	L/S/h	62	30	A
			F006	L/M/h	65	56	
			F007	L/F/h	61	77	
			F008	L/S/h	63	23	
			F009	L/S/h	60	24	
			F010	L/S/l	61	25	
6/7/85	Open field	Bell 206	F011	L/S/h	67	24	
			F012	L/M/h		54	
			F013	L/F/h		76	
			F014	H/S/h	73	25	
			F015	H/M/h	78	58	
			F016	H/F/h	72	80	
			F017	H/S/h	73	25	
			F018	H/M/h	75	58	
			F019	H/F/h	71	72	
			F020	L/S/h	58	36	
			F021	L/M/h	58	54	
			F022	L/F/h	59	71	
			F023	L/S/l	56	24	
			F024	L/M/l	59	60	
			F025	L/F/l	58	69	
6/8/85	Open field	Ag Husky	F027	L/S/h	65		
			F028	L/S/h	75	98	
			F029	H/F/h	91	122	
			F030	H/S/h	80	95	
			F031	L/S/h	69	96	
			F032	L/F/h	66	119	
			F033	H/S/h	86	92	
			F034	L/S/h	64	95	
			F035	L/S/l	64	91	
			F036	L/S/l	63	93	
			F037	L/S/l	65	95	
			F038	L/S/l	67	95	
			F039	L/S/l	68		
6/9/85	Open field	Ag Husky	F041	L/S/h	68	103	
			F042	L/F/h	67	116	
			F043	H/S/h	88	95	
			F044	L/S/h	65	99	
			F045	L/S/h	69	95	
			F046	L/F/h	69	110	
			F047	H/S/h	89	96	
			F048	L/S/l	63	92	
			F049	L/S/l	61	94	
			F050	L/S/l	62	94	
			F051	L/S/l	65	93	
			F052	L/S/l	62	92	
			F053	L/S/l	63	95	
			F054	L/S/l	62	95	
			F055	L/S/l	61	79	
			F056	L/S/l	61	80	
			F057	L/S/l	59	76	
			F058	L/S/l	61	80	
			F059	L/S/l	61	81	
			F060	L/S/l	63	75	

L = low; S = slow; M = medium; F = fast; H = high; h = heavy; l = light

TABLE 5-1 (Cont'd)

Date	Location	Aircraft	Flight No.	Description	Altitude (Ft)	Ground Velocity (mph)	Instrument Grid
6/14/85	Forest	Bell 206	F062	L/S/h	68		B
			F063	L/S/h	64		
			F064	L/F/h	72		
			F065	L/S/h	77		
			F066	H/M/h	79		
			F067	L/S/h	79		
			F068	L/S/h	69		
			F069	L/S/h	71		
			F070	L/S/h	72		
			F071	L/S/l	72	27	
			F072	L/S/l	77	44	
			F073	L/S/l	74	62	
			F074	L/S/l	67		
6/15/85	Forest	Bell 206	F076	L/M/l	66	55	C
			F077	L/F/l	67	83	
			F078	H/M/l	76	51	
			F079	H/M/l	73	68	
			F080	H/F/l	81	90	
			F081	L/S/l	65	40	
			F082	H/S/l	78	43	
			F083	L/S/l	68	36	
			F084	L/M/l	66	54	
			F085	L/F/l	71	69	
			F086	H/S/l	77	38	
			F087	H/M/l	86	62	
			F088	H/F/l	83	70	
			F089	L/S/l	64		
			F090	L/S/l	65	45	
			F091	L/M/l	67	55	
			F092	H/S/l	77	29	
			F093	H/M/l	82	44	
			F094	H/F/l	83	59	
			F095	L/S/l	66		
			F096	L/S/l	64	24	
			F097	L/S/l	63	24	
			F098	L/S/l	64	24	
6/16/85	Forest	Ag Husky	F101	L/F/h	85	115	B
			F102	L/S/h	76	96	
			F103	L/F/h	75	121	
			F104	H/S/h	110	95	
			F105	L/S/h	98	101	
			F106	L/S/h	87	101	
			F107	L/S/h	88	101	
			F108	L/S/h	86	96	
			F109	L/S/h	75	94	
			F110	L/S/l	74	94	
			F111	L/S/l	74	85	
			F112	L/S/l	83	93	
			F113	L/S/l	81	87	
			F114	L/S/l	81	74	
			F115	L/S/l	78	76	
			F116	L/S/l		78	
			F117	L/S/l		94	

TABLE 5-1 (Cont'd)

Date	Location	Aircraft	Flight No.	Description	Altitude (ft)	Ground Velocity (mph)	Instrument Grid
6/17/85	Forest	AG Husky	F119	L/S/h	76	98	C
			F120	L/S/h	70	96	
			F121	L/S/h	71	94	
			F122	L/F/h	70	119	
			F123	H/S/h	109	91	
			F124	L/S/h		91	
			F125	L/S/h	78	90	
			F126	L/F/h	76	103	
			F127	H/S/h	107	89	
			F128	L/S/l	73	96	
			F129	L/S/l	72	92	
			F130	L/S/l	73	93	
			F131	L/S/l	72	80	
			F132	L/S/l	77	76	
			F133	L/S/l	76	85	
			F134	L/S/l	72	82	
			F135	L/S/l	75	86	
			F136	L/S/l	73	78	
6/24/85	Orchard	Ag Cat	C003	F/h	40	98	D
			C004	F/h		98	
			C005	F/h		97	
			C006	F/h		96	
			C007	F/h		92	
			C008	F/h		97	
			C011	F/h		105	
			C012	F/h		95	
			C013	F/h		100	
			C014	F/h		96	
			C015	F/h		101	
			C016	F/h		95	
6/26/85	Orchard	Ag Cat	C019	S/h	40	78	D
			C020	S/h		80	
			C021	S/h		79	
			C024	F/h		91	
			C025	F/h		92	
			C026	F/h		95	
			C027	F/h		98	
			C028	F/h		95	
			C029	F/h		96	
			C032	F/h		94	
			C033	F/h		95	
			C034	F/h		93	
			C035	F/h		94	
			C036	F/h		96	
			C037	F/h		93	
			C038	F/h		95	
6/28/85	Orchard	Hiller 12E	C043	M/h	40		D
			C045	M/h		29	
			C046	M/h		32	
			C047	M/h		27	
			C048	M/h		29	
			C049	M/h		25	
			C050	M/h		25	
			C051	M/h		25	
			C052	M/h		26	
			C055	F/h		49	
			C056	F/h		48	
			C057	F/h		44	
			C058	M/h		25	
			C059	M/h		25	
			C060	M/h		25	
			C061	M/h		26	
			C062	M/h		24	
			C063	M/h		24	

TABLE 5-1 (Cont'd)

Date	Location	Aircraft	Flight No.	Description	Altitude (Ft)	Ground Velocity (mph)	Instrument Grid
7/2/85	Orchard	Hiller 12E	C068	F/h	40	45	D
			C070	M/h		20	
			C071	M/h		21	
			C072	M/h		23	
			C073	M/h		26	
			C074	M/h		24	
			C075	M/h		27	
			C076	M/h		25	
			C077	M/h		25	
			C078	M/h		26	
			C081	S/h		24	
			C082	S/h			
			C083	S/h		19	
			C084	S/h			
			C086	M/h		26	
			C087	M/h		22	
			C088	M/h		25	
			C089	M/h		24	
			C090	M/h		23	
			C091	M/h		26	
7/4/85	Orchard	Hiller 12E	C096	M/h	40	23	E
			C097	M/h		26	
			C098	M/h		25	
			C100	S/h		21	
			C101	S/h		19	
			C102	S/h			
			C104	F/h		35	
			C105	F/h		41	
			C106	F/h		39	
			C108	M/h		27	
			C109	M/h		28	
			C110	M/h		25	
			C111	M/h		26	
			C112	M/h		24	
			C113	M/h		24	
		Ag Cat	C117	F/h		94	
			C118	F/h		93	
			C119	F/h		94	
			C120	F/h		97	
			C121	F/h		95	
			C122	F/h		95	
			C123	F/h		93	
			C125	F/h		93	
			C126	F/h		95	
			C129	S/h		83	
			C130	S/h		80	
			C131	S/h		79	
7/6/85	Orchard	Hiller 12E	C136	S/h	40		E
			C137	S/h		19	
			C138	S/h		16	
			C139	S/h			
			C140	S/h		18	
			C141	S/h			
			C142	S/h			

6. DATA REDUCTION

6.1 Introduction

Wake flow field velocities were recorded from anemometers located at sixteen positions on a two-dimensional grid. The air velocity vectors at these locations, at instants in time, were displayed as snapshots of the flow field shortly after testing was concluded each day (Section 6.2). This provided a rapid evaluation of wake velocity signal strength and a preliminary indication of vortex pair behavior in each test. Merely displaying the direction and relative magnitude of the velocity vectors constructed from anemometer readings at each sensor location is not, however, a particularly useful method of characterizing a flow field for the purpose of modeling the wake-canopy interaction. To help quantify these data observations, a preliminary model of the aircraft wake was developed, coded and used to predict wake behavior in many of the field test runs. This section of the test report summarizes the model developed and presents conclusions about one such run. The next section of the report applies the techniques described here to the field test runs as the basis for drawing conclusions about the test series.

6.2 Flow Field Model

The preliminary model assumes that the aircraft wake may be represented by a simple vortex pair (with its image pair below the surface, Figure 6-1), each vortex of which adds a velocity field of the form

$$v = \Gamma/2\pi R \qquad (6\text{-}1)$$

where v = velocity magnitude,
Γ = vortex circulation strength, and
R = radius from vortex center.

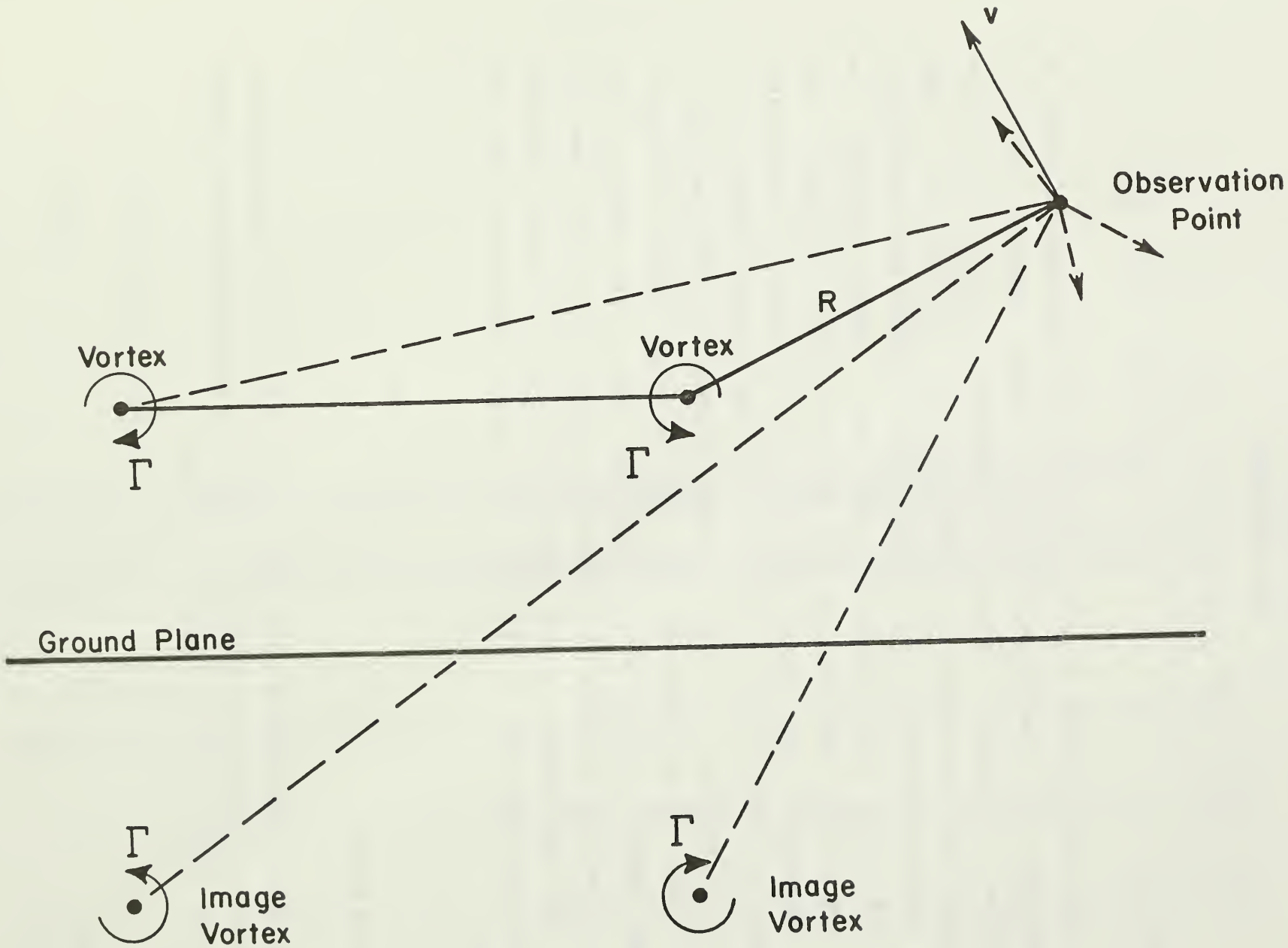

Figure 6-1. The composite velocity vector at an observation point found by summing the contributions of the aircraft vortex pair and its image system below the ground plane.

The total velocity at any point in the flow field (in particular, at a sensor location) in any run at any time, is then the algebraic sum of the velocity contributions from the four vortices acting on the flow.

The vortex pair must be located in a coordinate system relative to the tower grid (Figure 6-2). The aircraft wake model developed herein introduces four unknowns that must be deduced from the data in any run at any time increment at which data were collected. These unknowns are the vortex circulation strength and the three spatial dimensions (as shown in Figure 6-2) of

h = the height of the vortex pair above the surface,

s = the semispan of the vortex pair (the half distance between their centers), and

d = the offset distance of the aircraft centerline from the centerline of the tower grid.

When values are assumed for these four parameters, the velocity at every sensor can be computed and compared with the data recorded at that sensor. Since an aircraft flew over the tower grid to generate the data, it is presumed that a unique solution should exist for these four parameters. Of course, it is realized that the aircraft wake physics are only approximated by the simple velocity law imposed here. Thus, the intent of the analysis is to seek a solution for these four parameters in any run at every time increment so as to minimize the error in the velocity predictions at all of the sensors. With four unknowns and fifteen or sixteen sensor-locations, it seems clear that the problem may be cast into a least squares analysis to find the so-called "best fit" to the velocity data. This formulation, and its solution procedure, are discussed below.

6.3 Selection of Data to be Analyzed

The anemometer sensors provide both horizontal and vertical velocity time histories for up to sixty seconds after aircraft passage over the tower grid. These signals display the ambient wind before passage of the aircraft,

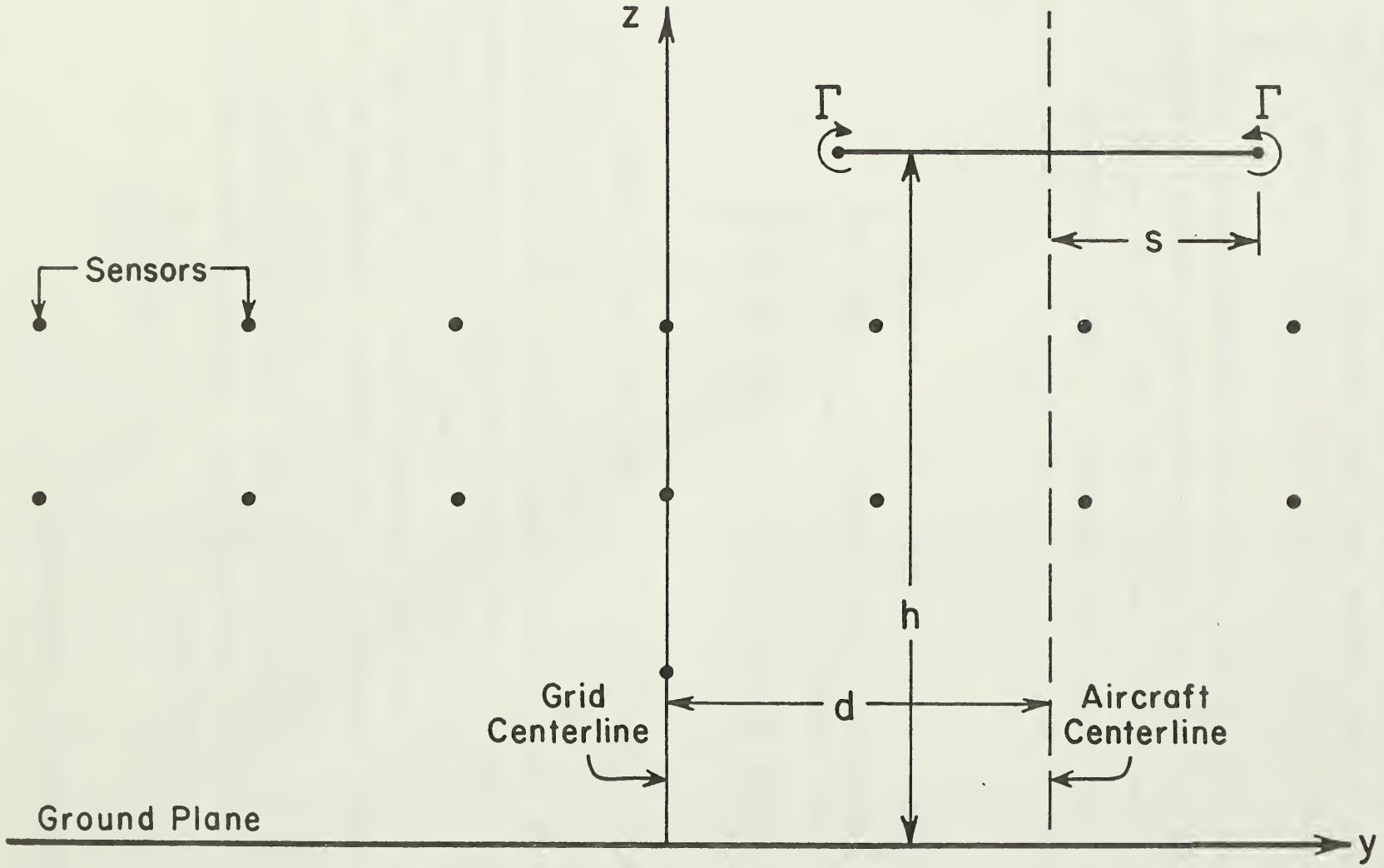

Figure 6-2. The aircraft vortex pair located relative to the sensor grid system. The relevant lengths are the height of the vortex pair h, the semispan distance between the vortices s, and the offset d of the aircraft centerline from the grid centerline.

then the signals generally increase substantially as the aircraft wake descends into the anemometer grid, decreasing later and returning to ambient conditions. A crosswind was present at the test site during most tests. Since the presence of this wind could dramatically alter the prediction of the aircraft wake, it was concluded that only the vertical velocity sensors would be used in the analysis, because this component is less responsive to ambient wind changes. Also, if the wake model is a good one, it is anticipated that the horizontal and vertical sensors would provide redundant information. An example later in this section will test this hypothesis.

It is true, however, that by the nature of the instruments used to measure the wind speed, a wind direction which is not exactly parallel to one of the sensors will invoke a correctible skewing error (Section 3.3). If only the vertical sensors are used in the analysis, an error in velocity magnitude as high as thirteen percent can result. Another example in this section evaluates this effect on the identification of the vortex pair.

6.4 Effects of Modeling Simplifications

The aircraft tested at Foresthill and Chico were helicopters in slow forward flight, a mono wing aircraft and a biplane. The wake model described in Section 6.2 contains only fully rolled-up tip vortices and assumes that the data to be analyzed are well away from the hover downwash effects of the helicopter, or in the case of the biplane well into the region where the two sets of vortices from each wing merge with each other. The adequacy of both of these assumptions may be verified by examining the relative error in cases where clear single vortex pairs were present, and in the first seconds of data where they were not. Additionally, as the aircraft wake descends into the canopy, several complicated processes tend to strip vorticity from the aircraft wake and alter the assumed vortex pair behavior dramatically.

For the example discussed in this section, however, only the flight over the open ground at Foresthill is examined, to present as clean a test configuration as possible.

6.5 Numerical Solution Procedure

The intent of the technique used to find the four unknowns in the aircraft wake model is to minimize the error between the actual velocity measured by the sensors and the predicted velocities of the model. The assumed error, E, may be defined as

$$E = \sum_{n=1}^{N} (w_n - \bar{w}_n)^2 \qquad (6\text{-}2)$$

where the overbar denotes the data, and the index, n, is from 1 to N, where N is the total number of sensors. The error, E, is a positive definite quantity. The vertical velocities, w, are determined by summing the contributions of the four vortices in the model (Figure 6-1), calculated for specific values of the parameters Γ, h, s and d. The data, $\bar{w}$, are read directly from the test results.

A crucial physical observation is made at this point; if the experimental data were normalized by any nonzero, positive value, the resulting velocity vectors could still be used to infer the spatial position of the vortex pair in the sensor field irrespective of the actual vortex circulation strength. This observation implies that locating the vortex pair involves the solution for h, s and d without reference to the value of Γ to determine where the vortices are positioned for minimum error.

The approach used here normalizes the vertical velocities in the error equation by the root mean square velocity (Eq. (6-4)). However, the predicted velocities are normalized by the predicted rms velocity, while the measured velocities are normalized by the rms of the measured velocities. If the technique described here is useful, it should be able to match rms values of predicted and measured velocities.

The error may then be rewritten in its normalized form as

$$E^* = \sum \left(\frac{w_n}{w_{rms}}\right) - \left(\frac{\bar{w}_n}{\bar{w}_{rms}}\right)^2 \qquad (6\text{-}3)$$

where

$$w_{rms} = \sqrt{\frac{1}{N}\sum w_n^2}$$

$$\bar{w}_{rms} = \sqrt{\frac{1}{N}\sum \bar{w}_n^2} \qquad (6\text{-}4)$$

Because the predicted vertical velocities are all linear in vortex circulation strength Γ, this modification to the error removes Γ from the equation for E^*, and recasts the problem into one involving the three parameters; h, s and d. The brute force approach to this problem is to calculate E^* for all combinations of the parameters h, s and d, and then to select that combination of values of h, s and d which minimizes E^*. This approach is computationally inefficient and would require a prohibitive amount of computational time. To overcome this difficulty the error minimization procedure is recast in terms of influence coefficients as explained below.

The equation for E^* is nonlinear in h, s and d. It can, however, be analytically differentiated with respect to these three unknowns to give

$$F_h = \partial E^* / \partial h$$

$$F_s = \partial E^* / \partial s \qquad (6\text{-}5)$$

$$F_d = \partial E^* / \partial d$$

Clearly, when all three derivatives F_h, F_s and F_d tend to zero, the slopes of E^* also tend to zero and E^* reaches a local minimum value. These three F functions are nonlinearly related to h, s and d. At any value set of (h,s,d), the local values of the F's may be determined

numerically to generate partial derivatives of the form $\partial F/\partial h$, $\partial F/\partial s$ and $\partial F/\partial d$ to construct the model equation for F (representing F_h , F_s and F_d) of

$$\Delta F = \frac{\partial F}{\partial h} \Delta h + \frac{\partial F}{\partial s} \Delta s + \frac{\partial F}{\partial d} \Delta d \qquad (6\text{-}6)$$

The partial derivatives in this equation are known as the influence coefficients. In this equation for any value of (h,s,d), values of the three partial derivatives and F may be generated. Since the solution at the minimum requires F to tend to zero, the left-hand side of the equation is specified by

$$\Delta F = - F \qquad (6\text{-}7)$$

The complete system for all three F equations may be seen to be a three-equation system for the values $(\Delta h,\Delta s,\Delta d)$ to add to the present values (h,s,d) to give new values $(h+\Delta h,s+\Delta s,d+\Delta d)$ to recompute E^* and drive the solution to a minimum. This iteration procedure is followed at each time frame in the test run being analyzed.

Once values for (h,s,d) have been determined, the original error equation, E , may be differentiated to give

$$F_\Gamma = \partial E/\partial \Gamma = 0 \qquad (6\text{-}8)$$

to find the minimum of E and determine Γ . This equation is solved easily because the equation for F is linear in Γ . With the solution in hand for (Γ,h,s,d), these values are used as initial guesses for the next time frame in the run being analyzed.

6.6 Representative Test Result

The example illustrated here is for run F058 at Foresthill (no canopy), flown by an Ag Husky with a semispan of 20.8 ft, a weight of 3000 lbf and a flight speed of 80 mph. For this case, the aircraft vortex circulation strength is estimated to be 300 ft^2/sec.

Figures (6-3) through (6-6) present the results of the data reduction analysis, showing the horizontal positions of the left and right vortices, the vertical position of the vortex pair, the vortex circulation strength and the solution error, respectively, as a function of test time. In examining these results, it should be noted that the large changes of vortex position and circulation strength within a few seconds is not considered to be physically meaningful. While further study of the sources of high frequency variability is required it is safe to say that it results from a combination of data inaccuracy, model simplifications and possibly the minimization process itself. In any case, large changes in any parameter over a three-second interval should be disregarded and a smooth function should be faired through these results.

It may be seen from Figure 6-3 that crosswind is present, and that the preliminary wake model tracks the vortex centers in their motion from right to left across the tower grid. The vortices are located closer together than predicted with AGDISP, with a separation distance of 30 ft throughout most of the run, while the span of the aircraft is a little over 40 ft. AGDISP assumes that the wing loading is rectangular and places the vortices at the tips of the wings. However, for this particular aircraft configuration (flaps down for runs F056 - F060) the wing loading was greater on the inboard section of the wing than on the outboard section. This will cause the vortices to roll-up at a lateral position inboard of the wing tips as observed in the data. Figure 6-4 shows that the pair drift towards the surface, while Figure 6-5 shows an increase in circulation followed by a gentle decrease. The initial increase in circulation may indicate that the vortices have not merged completely and that what is being measured is the result of a composite vortex pair. It is also true that the actual aircraft wake flow is much more

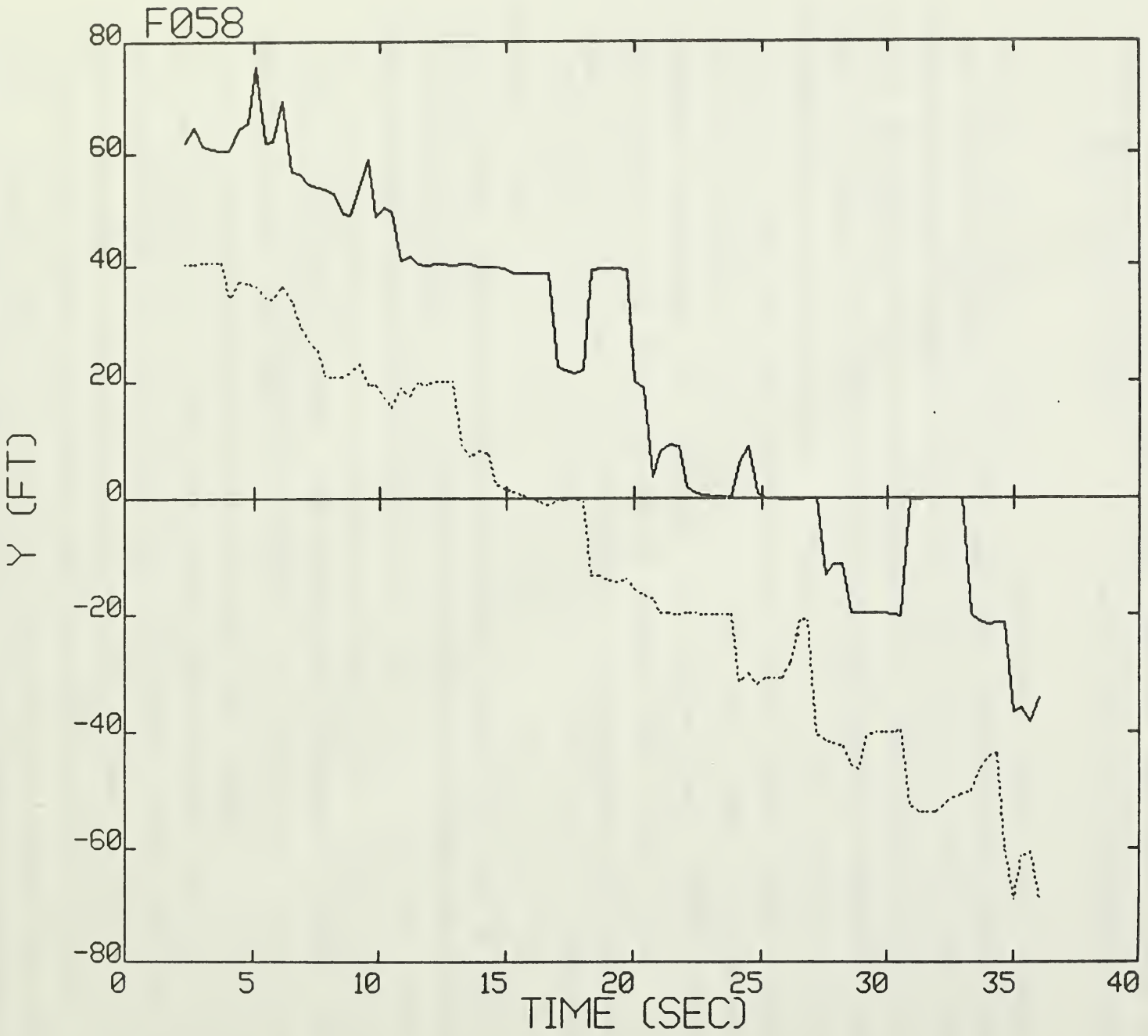

Figure 6-3. The predicted time history of the horizontal location of the right vortex (———) and left vortex (·····) in run F058.

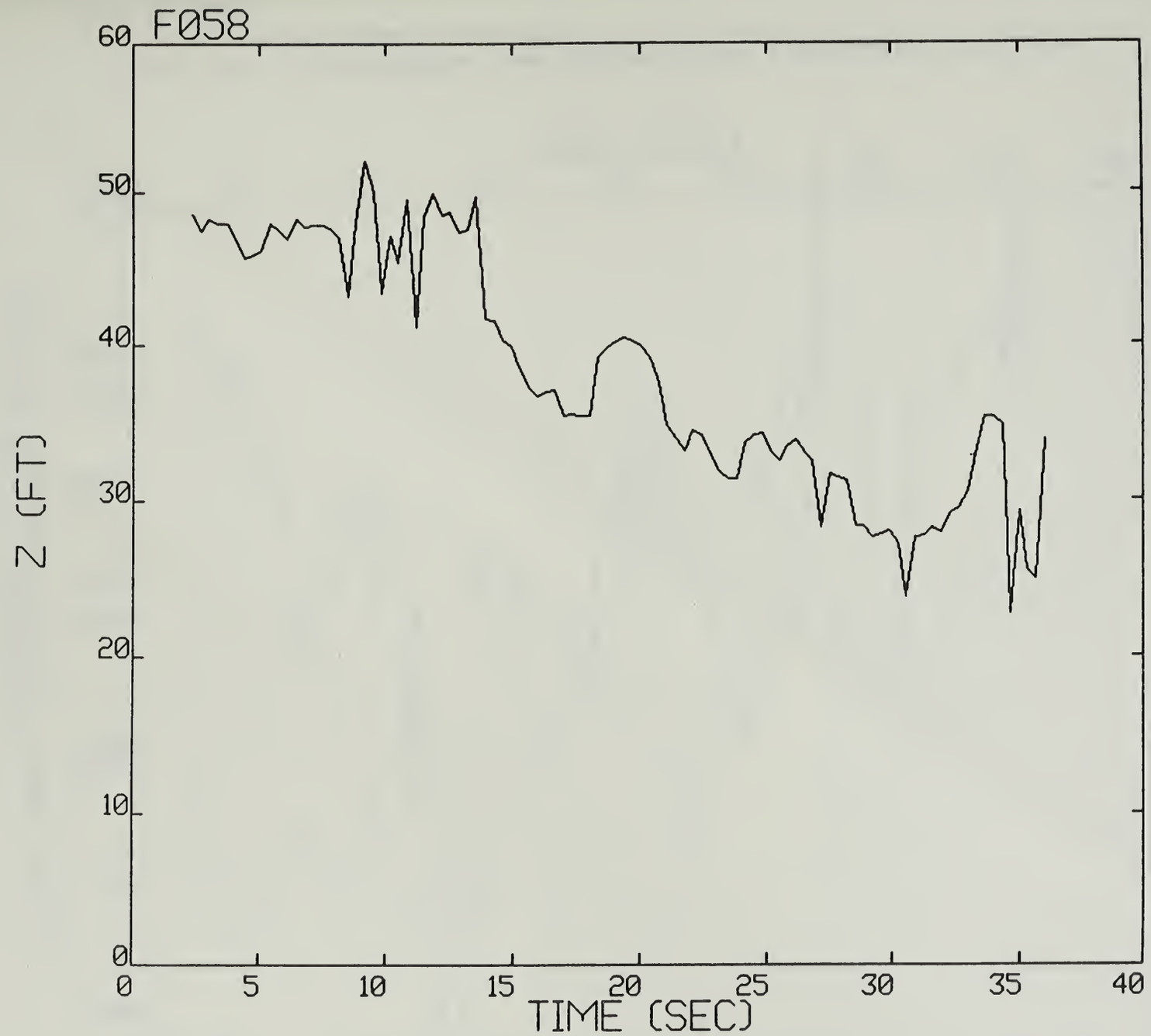

Figure 6-4. The predicted time history of the height of the vortex pair in run F058.

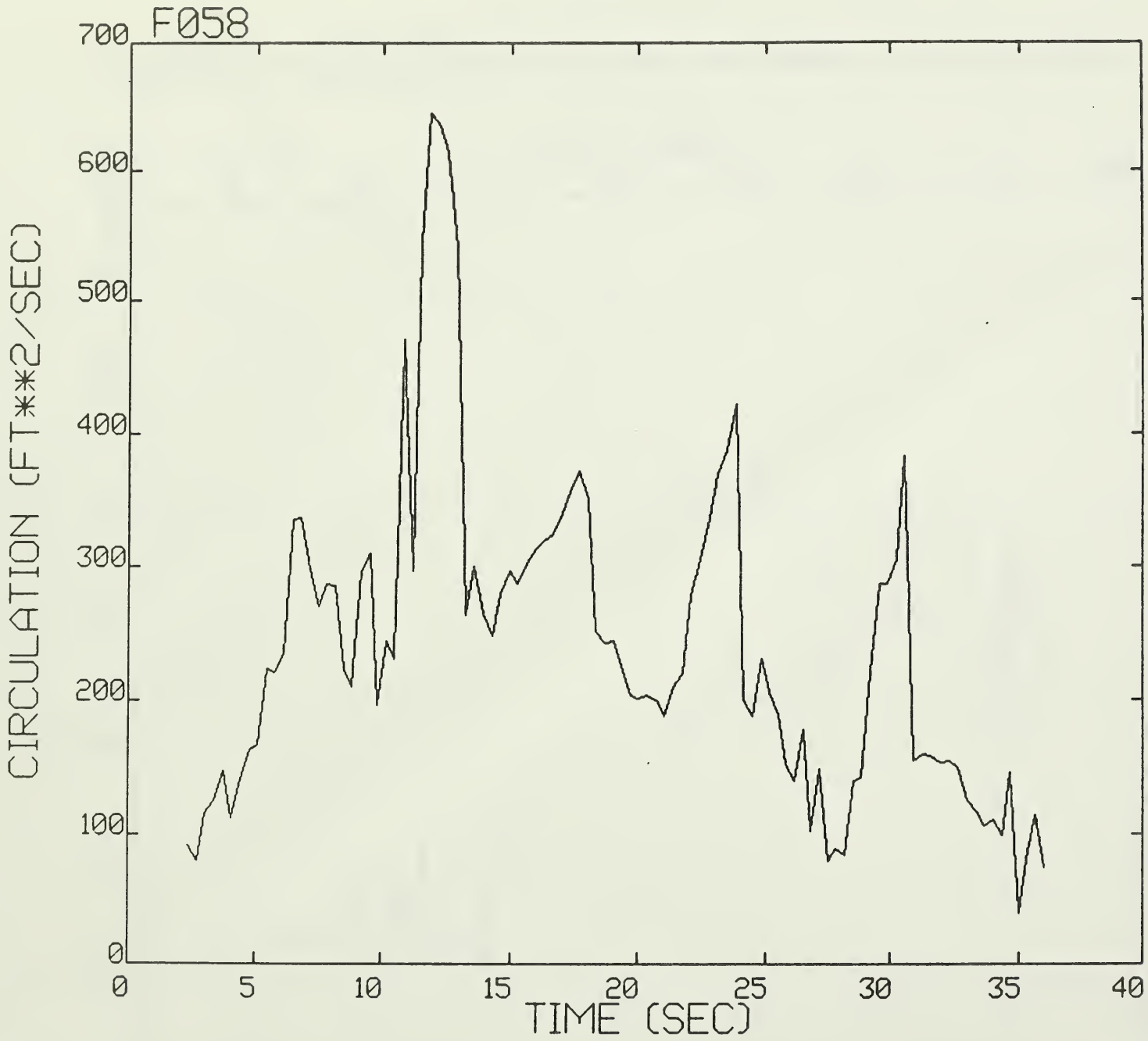

Figure 6-5. The predicted time history of the vortex pair circulation strength in run F058.

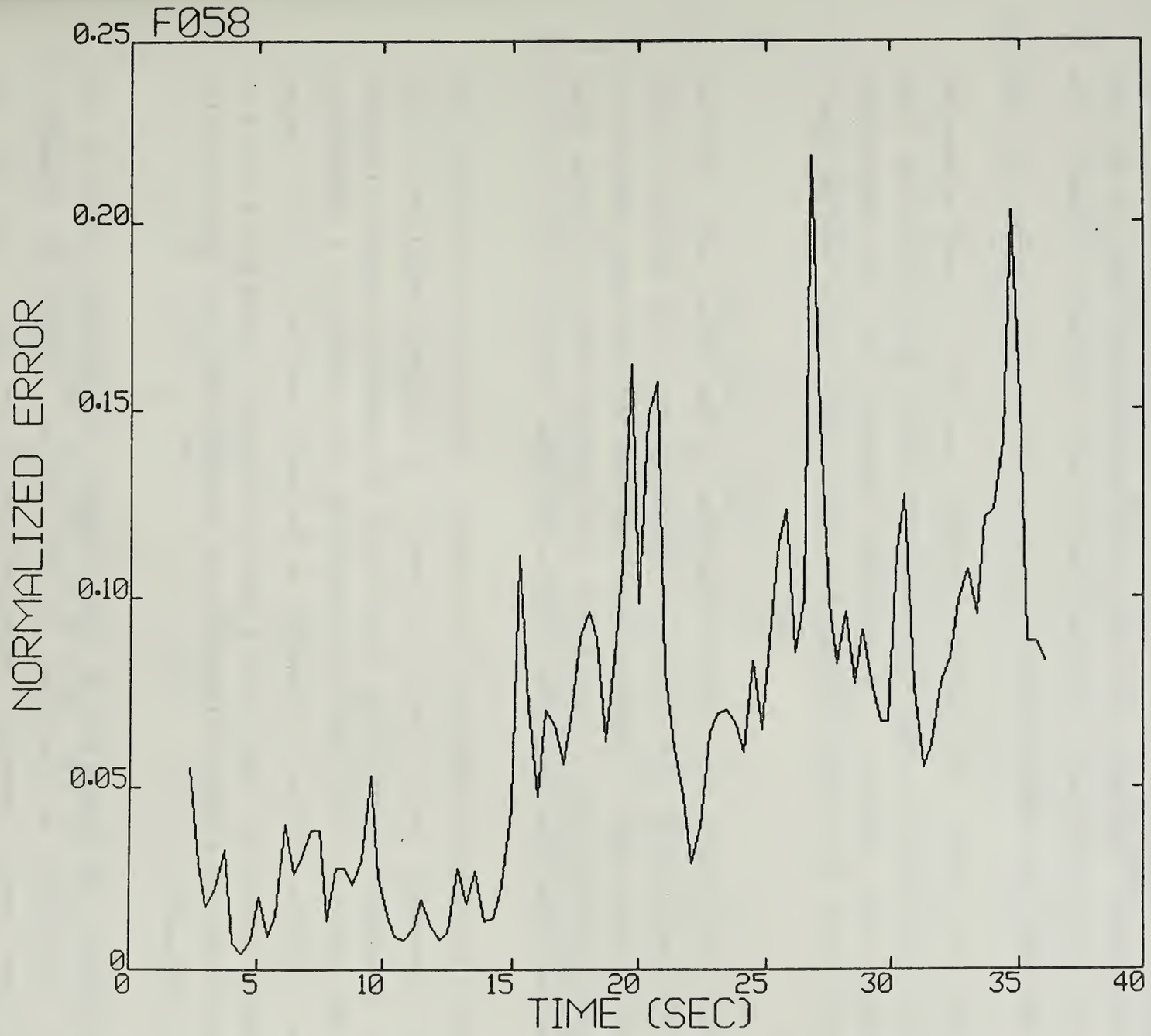

Figure 6-6. The time history of normalized error computed in run F058.

complicated than modeled here, and that atmospheric diffusion effects (also not modeled) diminish the vortex pair strength. Nonetheless, the results are encouraging.

Figure 6-6 presents the relative error, E , normalized by the error if the vortex circulation strength were zero, and demonstrates that as the run proceeded, the reduced sensor signals make it more difficult to predict the vortex pair parameters accurately.

Figure 6-7 presents the velocity vectors measured at each anemometer location at one instant in time. (This was the display generated in the field to evaluate data quality.) A snapshot excursion of the subsequently calculated vortex pair moving through the sensor field in run F058 is superimposed.

Figure 6-8 compares the spatial locations of the vortex pairs with and without the addition of the horizontal velocity data. The addition of the horizontal velocity data in these calculations does not alter the character of the results presented here, in particular when compared with the general level of variation of the time histories of these variables.

There is an error in measuring the vertical component of air velocity with a single anemometer due to the fact that it is slightly sensitive to the velocity component perpendicular to the axis of propeller rotation (Section 3.3). The effect of this error in identifying the location of a vortex pair is shown in Figure 6-9 and is observed to be small compared to other sources of parameter variance. Based on the results shown in Figures 6-8 and 6-9 it is concluded that in future tests most grid locations need only one vertically oriented anemometer.

In summary, the technique of least squares minimization based on the vertical velocities, as described in this section, appears to produce a reasonable and useful parametric representation of the data on run F058. It tracks the vortex centerlines with reasonable accuracy, descends as anticipated and initially has the right value of circulation. In the next section the results of applying this numerical technique to representative data collected during the scoping runs at Foresthill and Chico are presented.

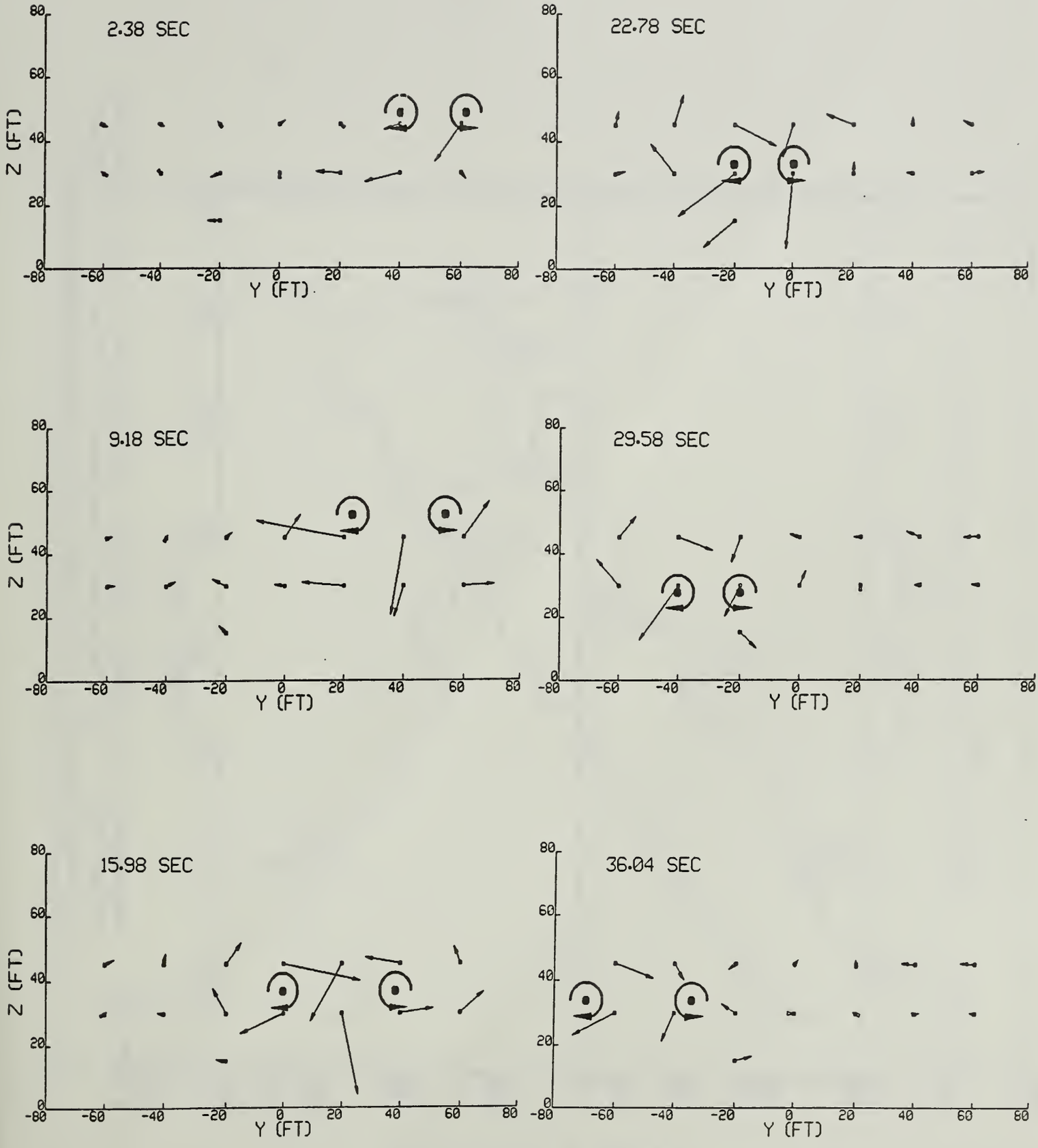

Figure 6-7. The predicted spatial position of the vortex pair at several times in run F058. The arrows represent the direction and relative strength of the velocity data at the times noted.

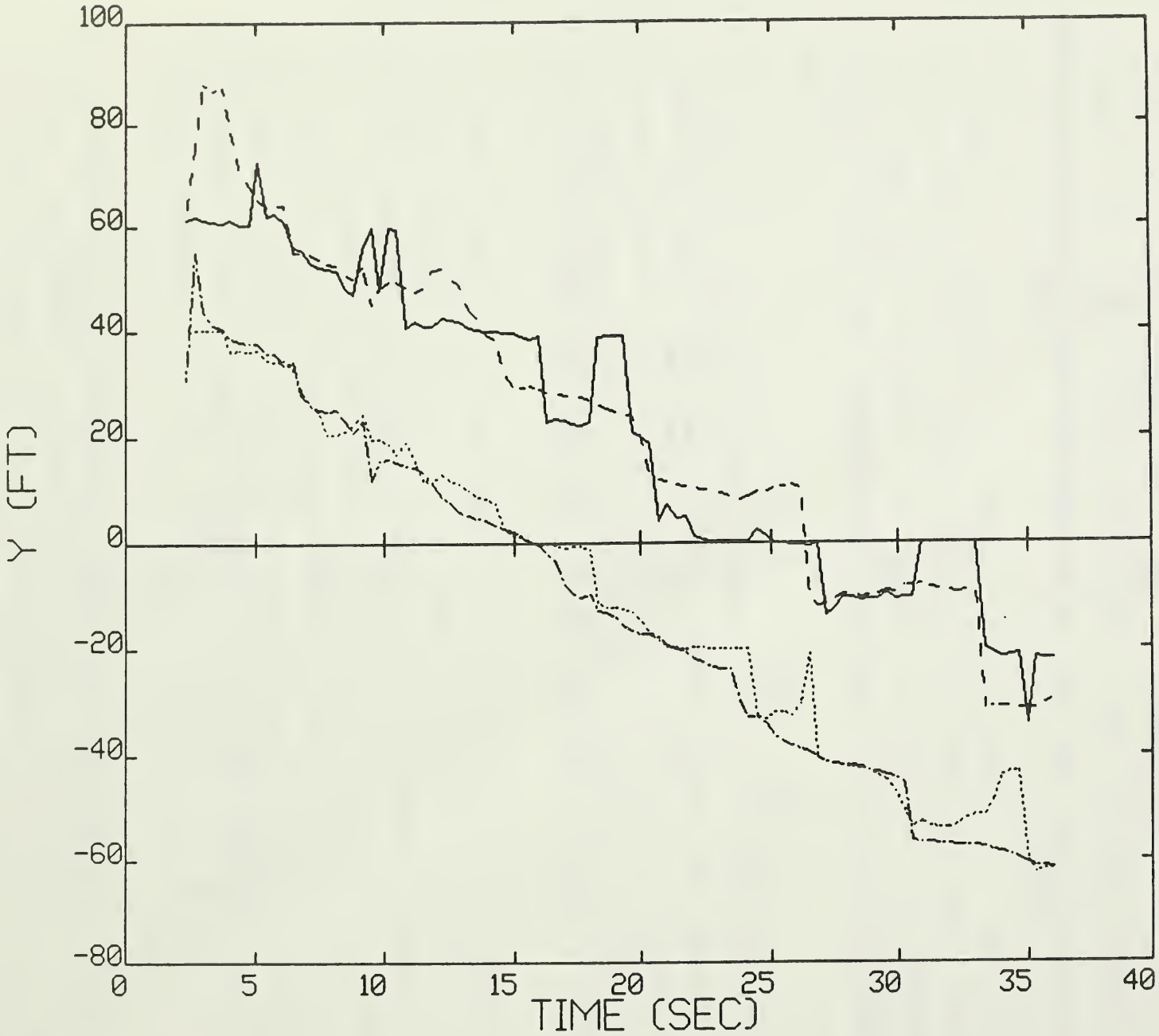

Figure 6-8. Comparison of the spatial location time histories for the vortex pair in run F058. a) Horizontal locations (———) and (·····) without horizontal velocity; (-----) and (-·-·-) with horizontal velocity.

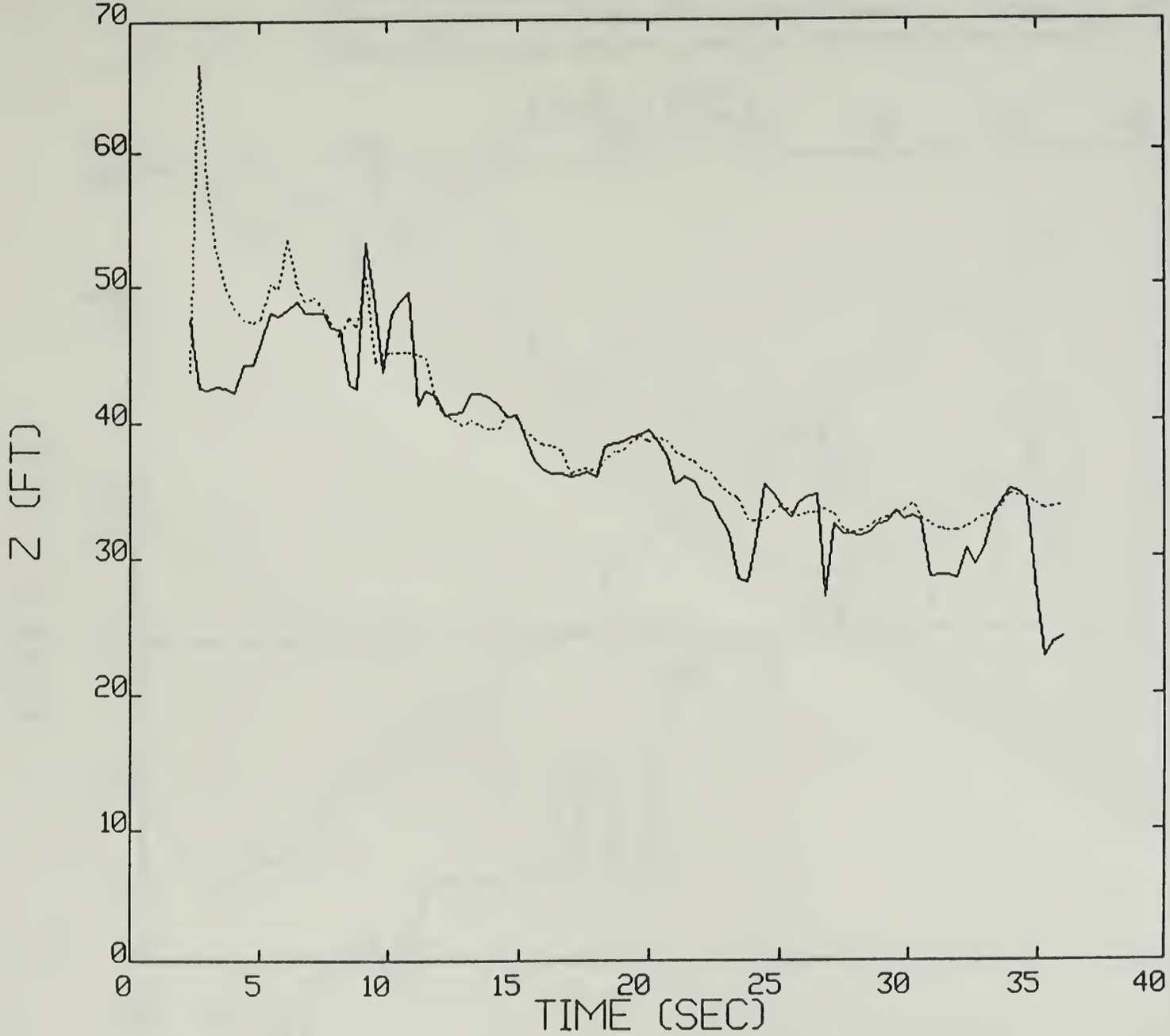

Figure 6-8b. Height (———) without horizontal velocity; (·····) with horizontal velocity.

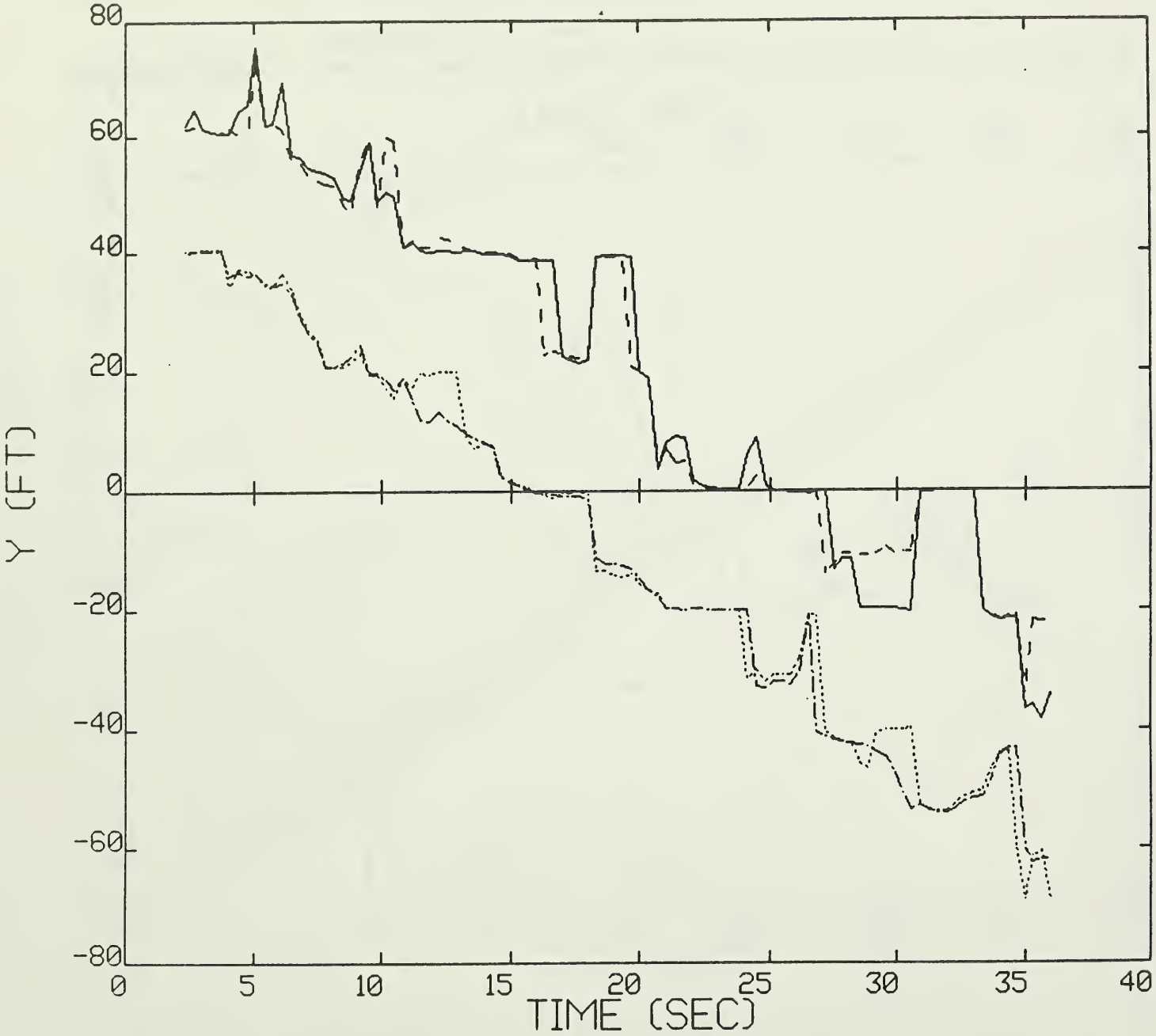

Figure 6-9. Comparison of the spatial location time histories for the vortex pair in run F058. a) Horizontal locations (———) and (·····) without anemometer correction; (- - -) and (-·-·-) with correction.

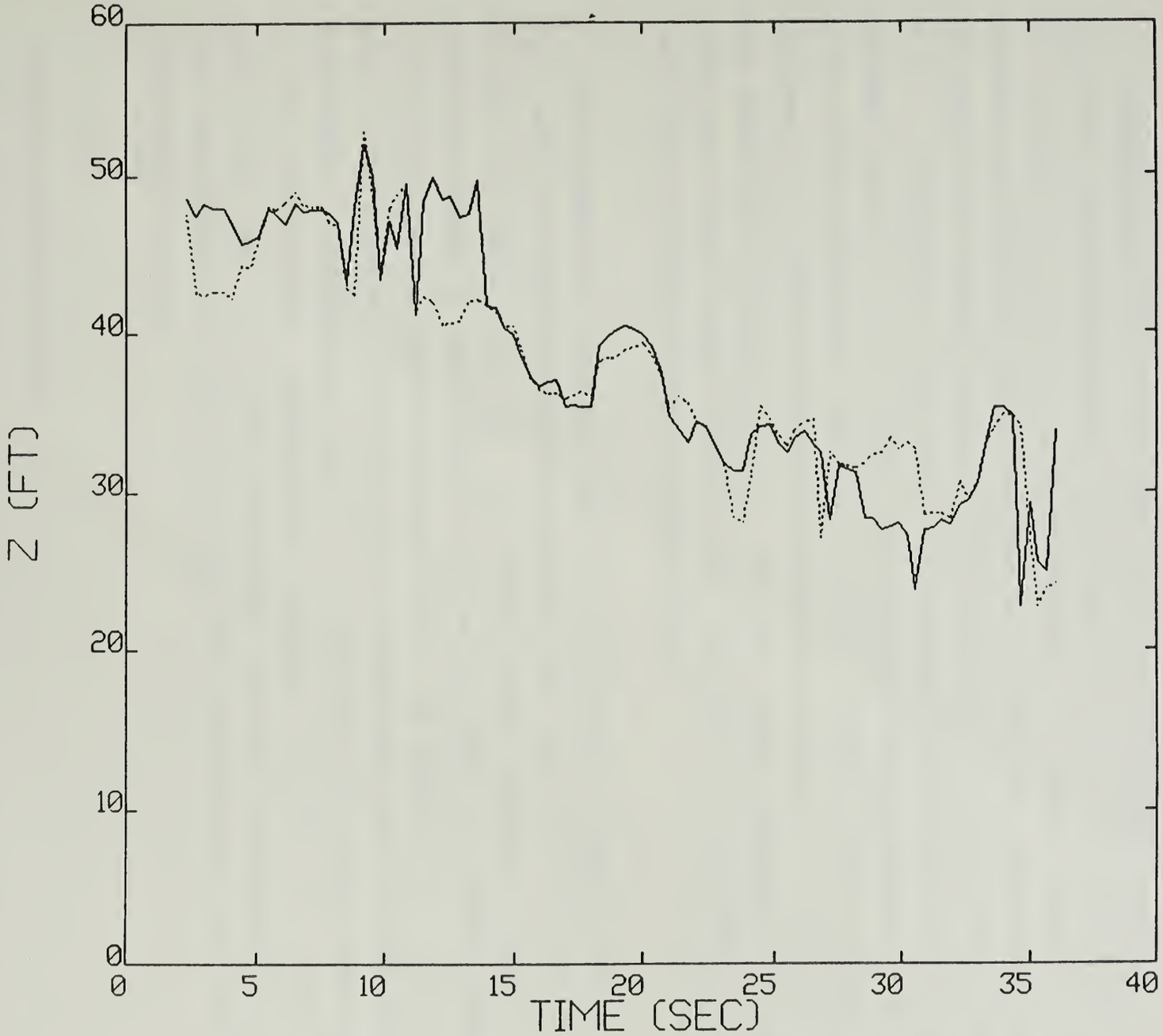

Figure 6-9b. Height of vortex pair (———) without anemometer correction (·····) with correction.

7. TEST RESULTS

7.1 Introduction

The primary objective of the test program is to evaluate the use of a two-dimensional grid of anemometers in studying the wake flow of an aircraft in the presence of forest and orchard canopies. The second objective is to ascertain the effect of forest canopies on the wake flow with an eye towards developing more effective techniques for penetrating the canopy with chemical sprays. A discussion of the results obtained and how well the objectives are achieved is given in this section. The baseline results obtained in the open field at the Foresthill site are presented. These results evaluate the instrumentation technique without the additional complexity of the canopy but with significant crosswinds present. Then the results obtained in the forest canopy and orchard canopy follow in that order with the fixed-wing aircraft test results preceding those of the helicopter.

It is generally concluded, based on the analysis of data to date, that this method of experimentally studying the wake flow field of a low flying aircraft is useful both with and without tree canopies. Based on the experience gained in this program, improvements would be made in anemometer orientation, and locations as discussed below. In addition, the mathematical model can be improved to more accurately represent the experimentally obtained flow field. The additional complexity of the model will require improvements in the iterative model identification technique presently used. Also, the present data base will provide researchers with ample opportunity to expand their understanding of the aircraft wake flow fields obtained with low flying agricultural aircraft.

7.2 Open Field Test Results

There were 58 flights flown by the Ag Husky and Bell 206 over the towers in the open field at different speeds, altitudes and weights. The aircraft generates the greatest circulation at the highest value of lift coefficient.

The runs chosen for presentation (Figure 7-1) are those flown with flaps down (highest lift coefficient) which are compared with theoretical predictions by the AGDISP computer code.[2] The predictions are based on aircraft altitude, velocity, weight and wing span.

As described in Section 6, the measured wake flow is parametrized in terms of a rolled-up inviscid vortex pair. Both vortices have circulation strength , Γ , and are located at altitude z . The lateral location, y , of the vortex on the right side of the aircraft is shown as a solid line in Figures 7-1 through 7-6. For the vortex on the left side of the aircraft, a dotted line is used. The origin of the y axis is at the middle tower. The origin of the time axis is when the operator initiated the data acquisition sequence. The predicted vortex circulation strength and locations are shown as dashed lines.

Results from flights F056 and F058 are shown in Figure 7-1. Both flights were at an altitude of 60 ft, velocities of 117 ft/sec, at the same weight and the same flap settings. The resulting flow fields should, therefore, be similar. These results are presented in order to evaluate the repeatability of the test results, as well as for comparison with computer predictions.

Several comments are in order prior to reviewing the test results. For evaluating repeatability, a shift of the time axis by several seconds is permissible due to variation in operator initiation of the test sequence. Also, the crosswind can be different for different runs thus altering the slope of the lateral vortex position time histories. Finally, the apparent rapid changes in these functions (one- to three-second intervals) should be averaged by eye (Section 6.6) so that the physically meaningfuly low frequency trends can be discerned and compared. With these comments in mind, the test results can now be reviewed.

The time histories of the circulation strength, and vortex positions are adequately repeatable from flight to flight, given the background atmospheric variations and pilot control inputs (Figure 7-1). Furthermore, the results are in good agreement with theoretical predictions for the fixed-wing aircraft as evaluated using the AGDISP code.

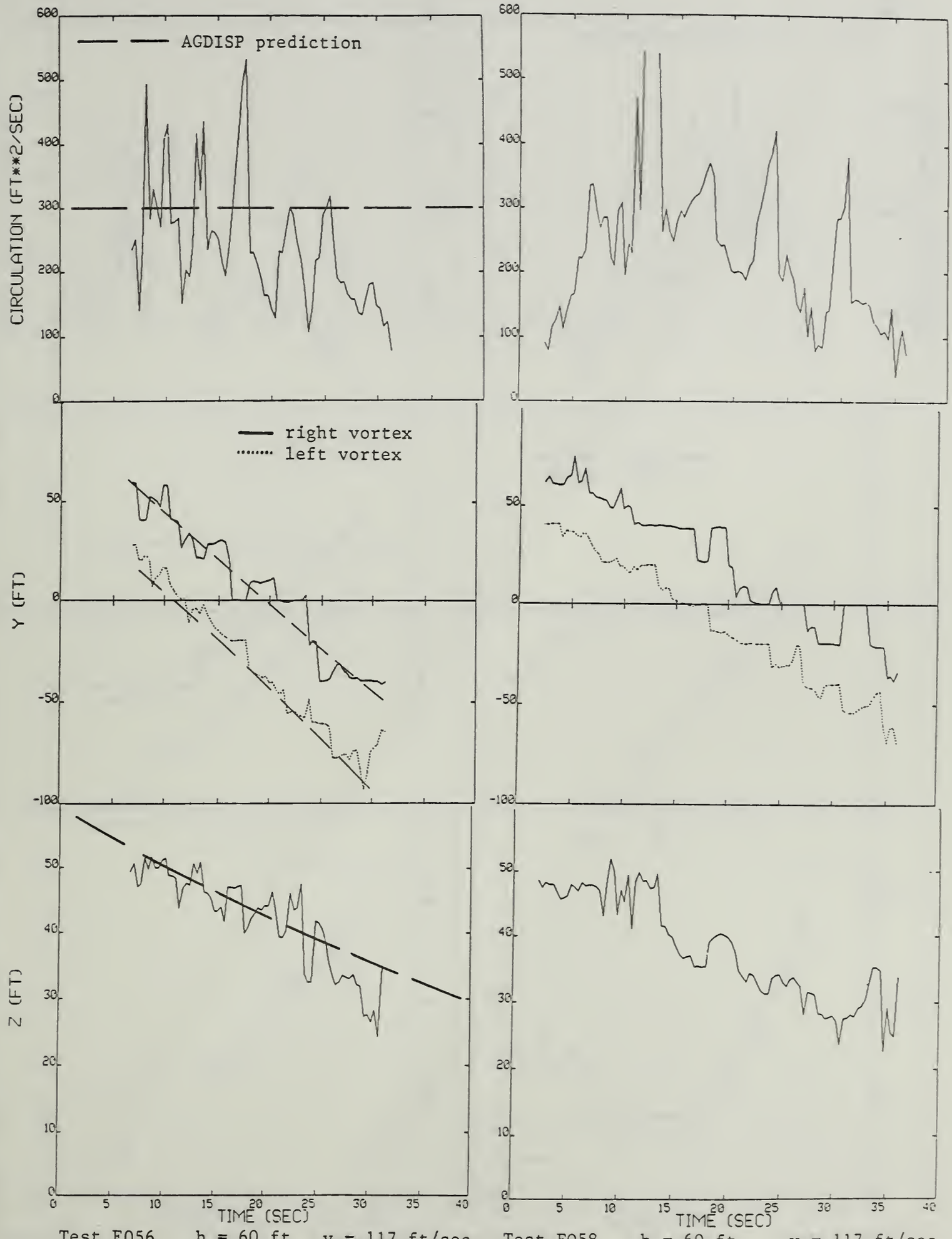

Test F056 h = 60 ft v = 117 ft/sec Test F058 h = 60 ft v = 117 ft/sec

Figure 7-1. Time histories of circulation and spatial positions of the vortex pair from open field for fixed-wing aircraft.

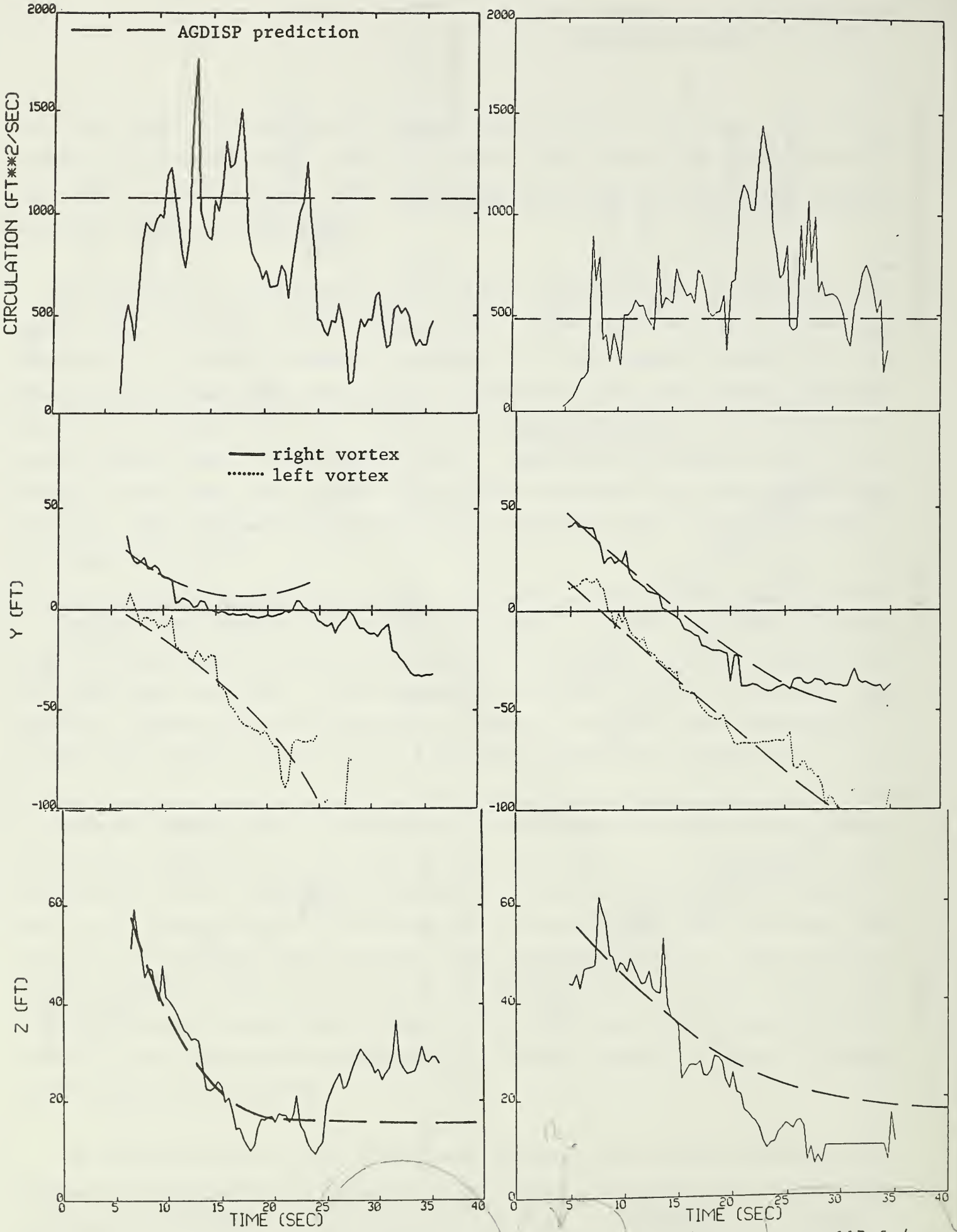

Test F009 h = 60 ft v = 117 ft/sec Test F058 h = 60 ft v = 117 ft/sec

Figure 7-2. Time histories of circulation and spatial positions of the vortex pair from open field for rotary-wing aircraft.

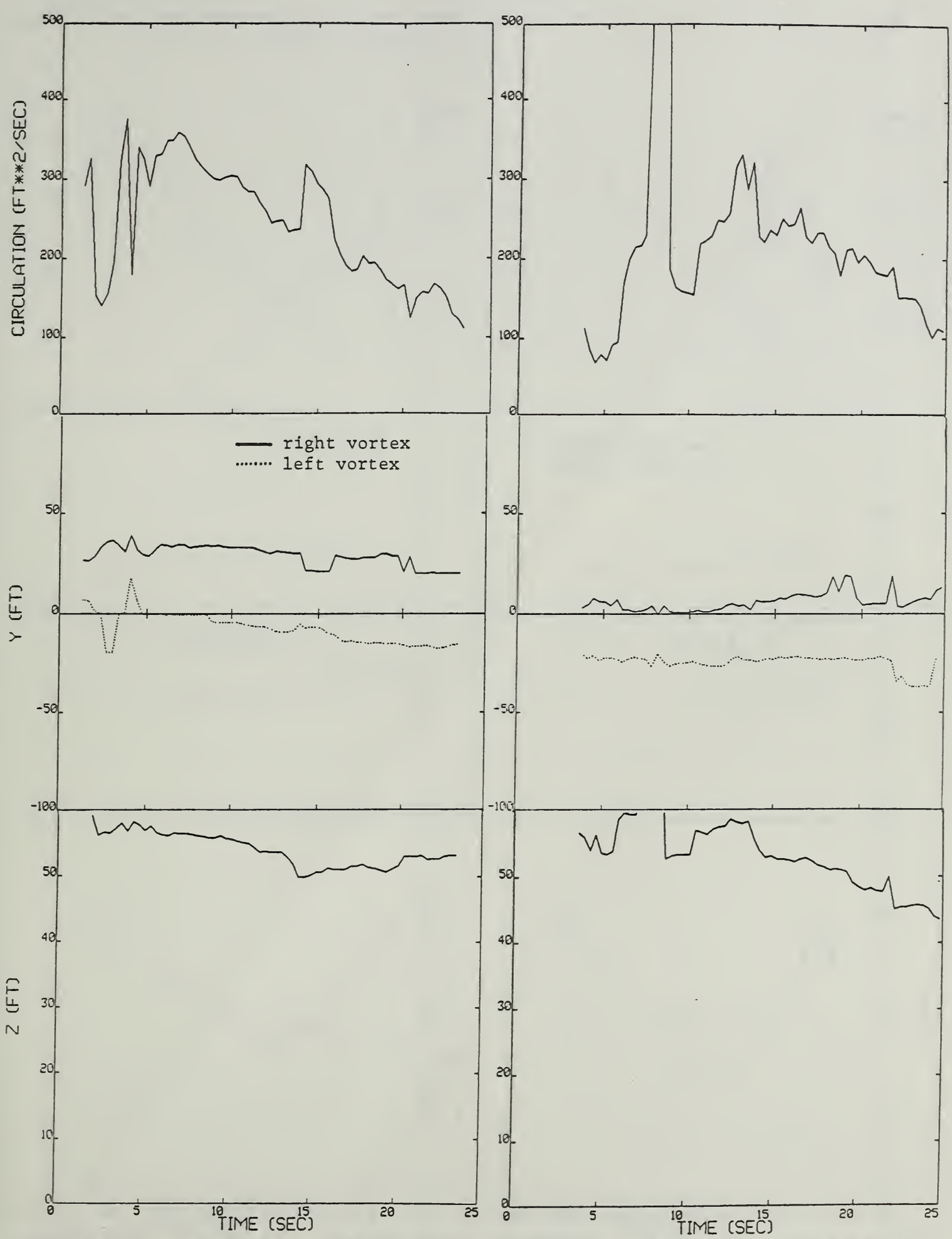

TestF121 h = 71 ft v = 138 ft/sec Test F125 h = 78 ft v = 144 ft/sec

Figure 7-3. Time histories of circulation and spatial positions of the vortex pair from forest site for fixed-wing aircraft.

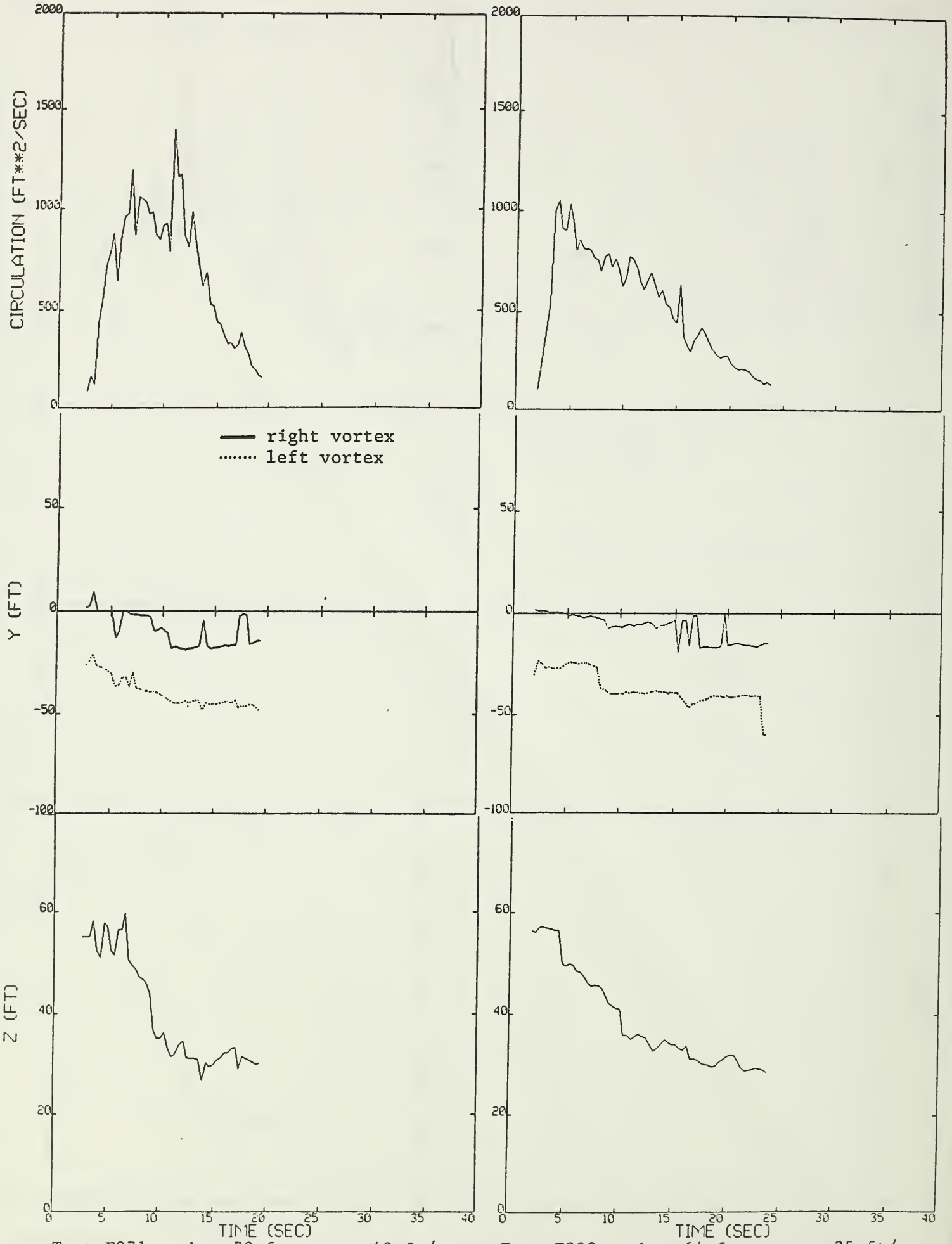

Test F071 h = 72 ft v = 40 ft/sec Test F098 h = 64 ft v = 35 ft/sec

Figure 7-4. Time histories of circulation and spatial positions of the vortex pair from forest site for rotary-wing aircraft.

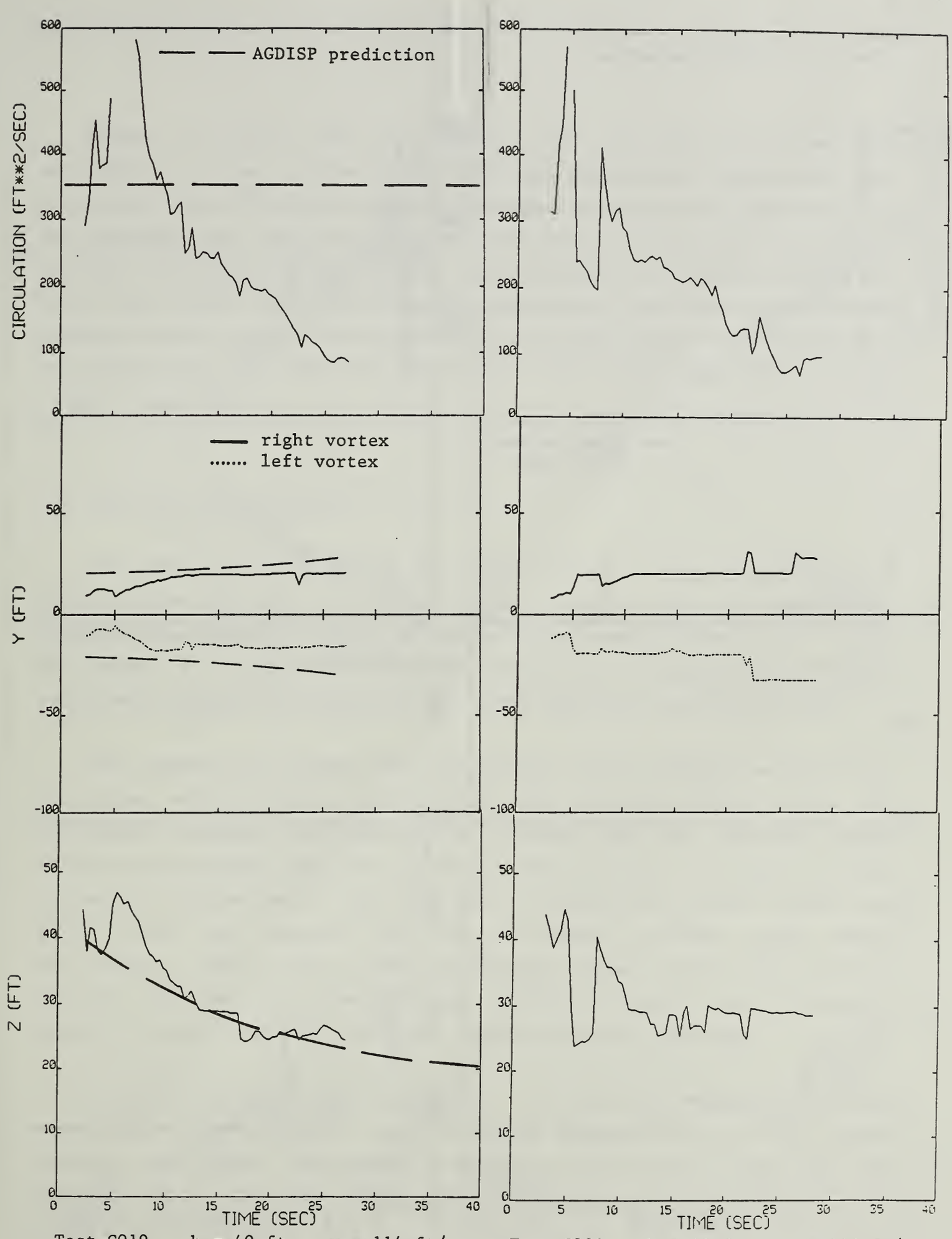

Test C019 h = 40 ft v = 114 ft/sec Test C021 h = 40 ft v = 116 ft/sec

Figure 7-5. Time histories of circulation and spatial positions of the vortex pair from orchard site for fixed-wing aircraft.

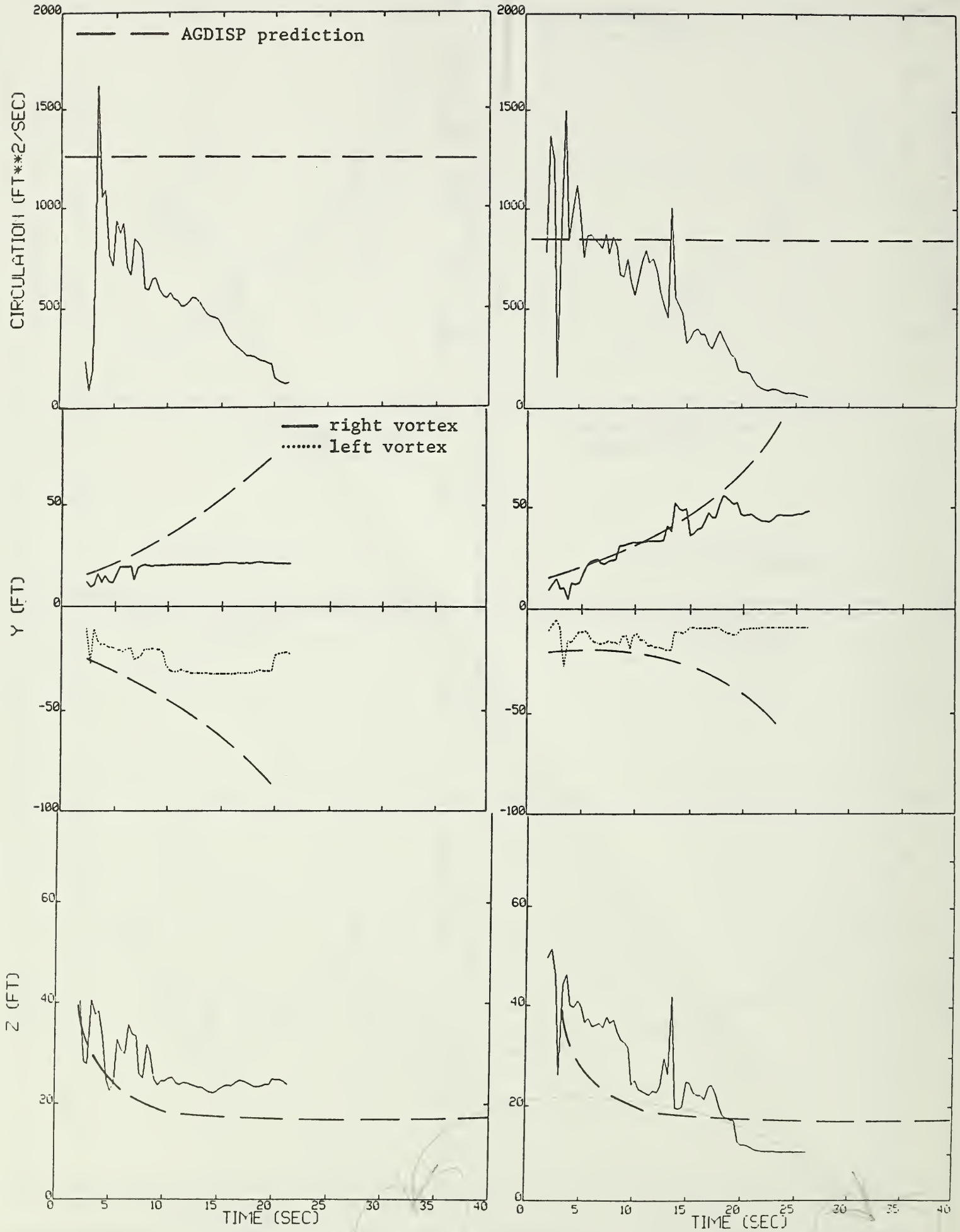

Test C098 h = 40 ft v = 28 ft/sec Test C101 h = 40 ft v = 37 ft/sec

Figure 7-6. Time histories of circulation and spatial positions of the vortex pair from orchard site for rotary-wing aircraft.

Results of flights over the towers in the open field by the Bell 206 helicopter are shown for two different flight velocities (Figure 7-2). In both cases, the circulation initially increases as vortex roll-up occurs. In the low speed case, the vortices descend and appear to bounce as they separate laterally and dissipate circulation. At 80 ft/sec the vortices descend and spread more slowly than theoretically predicted and the circulation strength remains slightly greater than predicted. In these cases, the calculation of the vortex pair stops when one vortex is too far away from the line of towers (-60 ft $\leq y \leq 60$ ft).

7.3 Forest Site Test Results

There were 71 overflights of the towers erected in the forest by the Ag Husky and the Bell 206. No attempt is made in this report to compare test results with theoretical models of vortex-forest canopy interaction. Rather the intent is to note the differences between the experimentally observed vortex pair strength and motion in the forest and in the open field sites.

Test results from flights F121 and F125 for the Ag Husky at velocities of 138 ft/sec and 144 ft/sec, respectively, are presented (Figure 7-3). The circulation strength is observed to decrease and the vortices remain relatively stationary near the top of the trees (50 ft). In these two cases parametric calculations of the flow field stop when the vortex centers are still within the towers, but the circulation strength drops below 100 ft^2/sec. This is due to the low velocity signals (less than 2 ft/sec) obtained with the 20-ft tower spacing. Vertical position and circulation strength are not shown for $t = 7$ sec because they are too large.

The same phenomenon ($\Gamma < 100$ ft^2/sec) also ends the calculation of test results with the helicopter over the forest (Figure 7-4). In this case, however, the initial circulation strength is much higher than with the Ag Husky due to the lower speed, and the vortices penetrate well into the canopy.

7.4 Orchard Site Test Results

There were 109 flights over the Hennigan Almond Orchard by the Schweizer Ag Cat and the Hiller UH-12E, all at an altitude of 40 ft. Flights C019 and C021 by the Ag Cat were at identical conditions with the anemometers in the top two rows (grid D, Figure 3-3) supplying the data (Figure 7-5). Theoretical predictions with no canopy are shown as a reference for these experimental data obtained in the orchard. As in the forest, the circulation strength dissipates with the vortices remaining near the top of the almond trees (25 ft). For these low strength vortices the instrumentation distribution of grid D gives better vortex identification than with grid E (Figure 3-3, there is not enough vortex penetration to produce good signals in the lowest row of instrumentation).

Test results from helicopter flights C098 and C101 at velocities 28 ft/sec and 37 ft/sec, respectively, are presented along with theoretical predictions with no canopy effects (Figure 7-6). In both cases, the attenuation of the circulation strength is significant, which in turn alters the path of the vortices.

8. CONCLUSIONS AND RECOMMENDATIONS

The primary objective of this test program is to demonstrate that a grid of anemometers can be used to obtain the data needed to develop an aircraft wake-canopy interaction model. The test program has demonstrated that the pair of vortices identified from the anemometer measurements in the open field agree well with analytic predictions. In addition, the anticipated dissipation of the vortices by the interaction with the canopy has been confirmed by the anemometer data. The primary objective of this test program has, therefore, been attained.

The vortex pair generated by the helicopter at slow forward speeds penetrated well into the coniferous and broadleaf canopies. The vortex pair generated by the fixed-wing aircraft having considerably less circulation strength than that generated by the helicopter did not penetrate deeply into either canopy tested.

It is recommended for further testing that the anemometer grid be extended laterally (more towers) in order to track the wake for a longer duration under normal operating crosswind conditions. It is also desirable to mount most of the anemometers vertically, since the ambient crosswind component, which produces errors in the identification of vortices, is greater in the horizontal direction. The maximum number of anemometer signals which could be measured and recorded for each flight of this test program was limited to 32 by the DAS. It is recommended that a 60+ channel DAS be used and with higher sampling rate so that the grid spacing can remain fine enough to resolve circulation strengths of 100 ft^2/sec anywhere in the laterally extended grid suggested above. With these improvements in experimental technique it should be possible to obtain higher quality data which will ultimately result in more accurate modeling of the wake-canopy interaction.

The data reduction algorithm developed in this program identifies the circulation strength and position of a vortex pair. This algorithm should be extended to identify more parameters associated with more complex flow

fields. These include: improved vortex core models, unequal strength vortices which can rotate about each other, and the nonvortex lift associated with a rotor at low advance ratios.

A total of 238 flights were made over the anemometer grids of which 36 have been analyzed. Not all of the unanalyzed data are equally useful due primarily to high gusty crosswinds, but the majority of the data still remain to be analyzed and used in the further development of wake-canopy models. This would logically follow after the data reduction algorithm had been developed to identify the parameters of more realistic wake flow models.

9. REFERENCES

1. Honing F. and Holt Howard: "Test Plan for USDA Forest Service - DOD U.S. Army Cooperative Field Study Program WIND (Winds in Nonuniform Domains)" prepared by USDA Forest Service and Atmospheric Sciences Laboratory.

2. Bilanin, A.J. and Teske, M.E.: "Numerical Studies of the Deposition of Material Released from Fixed and Rotary Wing Aircraft," NASA CR Report No. 3779, March 1984.

3. Dumbauld, R.K., Bjorklund, J.R. and Saterlie, S.F.: "Computer Models for Predicting Aircraft Spray Dispersion and Deposition Above and Within Forest Canopies: User's Manual for the FSCBG Computer Program," H.E. Cramer Company, Inc. Report No. 80-11, 1980, pp. 270.

4. Teske, M.E.: "Computer Program for Prediction of the Deposition of Material Released from Fixed and Rotary Wing Aircraft," NASA CR Report No. 3780, March 1984.

5. Teske, M.E.: "User Manual Extension for the Computer Code AGDISP - Mod 3," prepared for the USDA Forest Service, Continuum Dynamics, Inc. Tech Note No. 84-5, May 1984.

6. Morris, D.J., Croom, C.C., Holmes, B.J. and van Dam, C.P.: "NASA Aerial Applications Wake Interaction Research," Paper No. AA-82-005 presented at the 1982 Joint Technical Session of the American Society of Agricultural Engineers and the National Agricultural Aviation Association, Las Vegas, Nevada, 1982.

7. Hallock, J.N. and Eberle, W.R.: "Aircraft Wake Vortices: A State-of-the-Art Review of the United States R&D Program," Department of Transportation Report No. FAA-RD-77-23, February 1977.

8. Burnham, D.C., Hallock, J.N., Tombach, I.H., Bradshears, M.R. and Barber, M.R.: "Ground-Based Measurements of the Wake Vortex Characteristics of a B-747 Aircraft in Various Configurations," Department of Transportation Report No. FAA-RD-78-146, December 1978.

9. Burnham, D.C.: "B-747 Vortex Alleviation Flight Tests: Ground-Based Sensor Measurements," Department of Transportation Report No. FAA-RD-81-99, January 1982.

10. Yates, W.E., Ogawa, J.M. and Akesson, N.B.: "Spray Distributions in Peach Orchards from Helicopter and Ground Applications," Transactions of the ASAE, Paper No. 68-617, 1974.

11. Butterfield, J.E. and Alliman M.A.: "Operations Plan for DOD US Army - USDA Forest Service Cooperative Field Study Project WIND (Winds in Nonuniform Domains)" prepared by Atmospheric Sciences Laboratory, May 1985.

12. "Operations Plan for Cooperative Field Study on Penetration of Aerial Sprays Into a Broadleaf Canopy," U.S. Department of Agriculture Forest Service and U.S. Army, STEDP-MT-DA-CB, June 1985.